Imaging Spectrum of Benign Uterine Disease and Treatment Options

Stephanie Nougaret, Martina Sbarra, Jessica Robbins

Imaging Spectrum of Benign Uterine Disease and Treatment Options

Stephanie Nougaret[1,2] MD, PhD; Martina Sbarra[3,4] MD; Jessica Robbins[5]

1. Montpellier Cancer Research Institute, INSERM, U1194, University of Montpellier, Montpellier, France. stephanienougaret@free.fr.

2. Department of Radiology, Montpellier Cancer Institute, , 208 Ave des Apothicaires, 34295, Montpellier, France.

3. Radiologia Diagnostica e Interventistica Generale, Dipartimento Diagnostica per Immagini, Radioterapia Oncologica ed Ematologia, Fondazione Policlinico Universitario A. Gemelli IRCCS, Rome, Italy.

4. Istituto di Radiologia, Università Cattolica del Sacro Cuore, Largo A. Gemelli 1-10123 Milano, Rome, Italy

5. University of Wisconsin School of Medicine and Public Health, 750 Highland Ave., Madison, WI, 53705, USA.

Nothing to disclose

Corresponding author:

Dr S. Nougaret, Department of Radiology, Institut du Cancer de Montpellier, 208 Rue des Apothicaires, 34 298 Montpellier, France (e-mail: stephanienougaret@free.fr)

Imaging Spectrum of Benign Uterine Disease and Treatment Options

Key words:

Leiomyoma; Leiomyosarcoma; Adenomyosis, MRI, Uterus

Key points:

- Benign uterine disease is mainly comprised of adenomyosis and leiomyomas, common gynecologic conditions affecting women of all ages.
- Magnetic resonance imaging (MRI) is the most accurate imaging modality for detection and localization of benign uterine disease and their mimics.
- MRI is the diagnostic tool of choice for pretreatment evaluation, assessing potential procedural risk and predicting treatment response, and monitoring treatment outcomes.

Abstract:

Benign uterine diseases are very common gynecologic conditions affecting women of all ages. Ultrasound is traditionally the first line imaging technique but patients are increasingly referred to magnetic resonance imaging as it is more accurate for diagnosis and patient management.

In this review, we will highlight the added value of magnetic resonance imaging in the diagnosis of the most common benign uterine diseases, describe therapeutic options, and delineate the role of MRI in treatment planning.

Introduction:

Benign uterine disease, such as adenomyosis and leiomyomas, are common gynecologic conditions affecting women of all ages[1-6]. Although ultrasound (US) is the first line imaging technique in the examination of the uterus, magnetic resonance imaging (MRI) has become very useful and is the most accurate tool in lesion diagnosis and patient management[7-13]. Indeed, benign uterine disease may manifest with atypical features and can mimic malignancy, making the correct diagnosis a challenge[10,14,15]. MRI also assists in the triage of symptomatic patients to the most appropriate treatment modality, including surgery (hysterectomy or myomectomy), interventional procedures (uterine artery embolization) and medical therapy[16-18]. Hysterectomy is curative, but uterus-sparing therapies are a valid alternative for eligible women.

In this article we highlight the utility of MRI in the diagnosis of the most common benign uterine diseases, such as leiomyomas and adenomyosis, discuss their typical and atypical MRI findings, describe the therapeutic options, and delineate the role of MRI in treatment planning.

MRI Protocol:

Clinical guidelines for diagnosis and management of patients with leiomyomas are extensive [1,19,20]. Recently, recommendations for MRI were proposed by the European Society of Urogenital Radiology[13].

Patient Preparation:

Fasting and the use of an antiperistaltic agent such as Buscopan or glucagon is useful to minimize motion artifacts related to small bowel peristalsis. A moderately full bladder is recommended to reduce artifacts related to bladder filling[13].

Imaging Protocol

High resolution thin-section images acquired at 1.5 T or 3.0 T are recommended.

The optimal protocol, according to recent ESUR guidelines is summarized in table 1[13].

Leiomyomas

Epidemiology, pathophysiology:

Leiomyomas are the most common benign uterine tumor affecting up to 20-30% of reproductive-aged women[11]. They are benign neoplasms of unknown cause composed of multiple layers of smooth muscle fascicles and fibrous connective tissue anchored in the muscular wall of the uterus. These tumors may be solitary or, most frequently, multiple [21]. The size of leiomyomas is variable and influenced by estrogen and progesterone; they often grow during pregnancy and with oral contraceptive use and regress after menopause [21]. They may be asymptomatic but 20-50% of women with leiomyomas present with symptoms such as menorrhagia, dysmenorrhea, pressure, urinary frequency, pelvic and back pain, and dyspareunia [5].

Location:

Leiomyomas generally involve the myometrium of the uterine corpus and are classified by their location as submucosal, intramural and subserosal. In accordance with the FIGO classification system, they can be further subdivided in 8 categories **(Figure 1)**[22]. Pedunculated lesions can become detached from the uterus, receiving blood supply from other adjacent structures, and are called "parasitic" leiomyomas[23,24]. Leiomyomas not related with the myometrium may be located in the cervix and in the round or broad ligaments.

Leiomyomas may occur in unusual locations such as diffuse peritoneal leiomyomatosis, intravenous leiomyomatosis or benign metastasizing leiomyoma. Peritoneal leiomyomatosis is characterized by multiple lesions along the peritoneal surfaces probably due to the iatrogenic dissemination throughout the peritoneal cavity after surgery [25]. A previous history of hysterectomy for leiomyomas or a diagnosis of uterine leiomyomas may point to the correct diagnosis. Intravenous leiomyomatosis has an aggressive intravascular growth pattern within intrauterine and systemic veins [25].

Imaging features

Ultrasound:

Ultrasound (US) is usually the initial imaging study.

On US, a typical leiomyoma is a well-defined mass, often shadowing at the margin and/or producing internal linear shadowing. The echogenicity varies from hypo to hyperechoic in relationship to the myometrium. Dystrophic calcifications can be seen particularly in postmenopausal women. On color - Doppler US, circumferential blood flow around the lesion is often seen [26].

MRI:

US can be limited by co-existing pelvic diseases, uterine anomalies, unusually small or large tumors, and tumor location [27]. Thus, MRI is considered the most accurate imaging modality to

detect, locate and characterize myometrial lesions prior to patient management [14,28]. MRI has reported sensitivities and specificities of 94.1% and 68.7%, respectively, for uterine leiomyomas[21,27,29].

On MRI, most leiomyomas, without any degeneration, are easily recognized as well-delineated round or ovoid lesions homogeneously hypointense on T2WI related to the outer myometrium and isointense on T1WI, with heterogeneous and variable enhancement. The presence of a T2-hyperintense rim indicates a pseudocapsule of edema due to dilated lymphatic vessels and veins [29] (Figure 2). Typical leiomyomas do not have restricted diffusion, showing a low signal intensity both on diffusion weighted images (DWI) and on the corresponding apparent diffusion coefficient (ADC) map, as a "blackout phenomenon" [10](Figure 2).

Two particular subtypes of leiomyoma have to be mentioned:

Cellular leiomyoma is a histological subtype characterized by more compact smooth muscle cells with little or no collagen; on MRI it shows higher signal intensity on T2WI and avid enhancement[11](Figure 3). The intermediate T2 signal and avid enhancement of cellular leiomyomas can make it difficult to differentiate them from leiomyosarcoma[30](Figure 3). In a retrospective study of 51 patients with a single myometrial lesion at MRI, Thomassin-Naggara et al suggested that the evaluation of DWI and ADC (value cut-off 1.23 x 10^{-3} mm^2/s) may limit the misdiagnosis of uterine sarcoma as leiomyoma with diagnostic accuracy of 92.4% [31] (Figure 3).

Lipoleiomyoma occurs in 0.03-0.2% of women, generally in the post-menopausal population. Liopleiomyomas are comprised of smooth muscle, adipose and fibrous tissue. The signal intensity of the fat components is typical high signal on T1WI and T2WI and loss of signal intensity on fat-saturated sequences [10].

When leiomyomas enlarge and outgrow their blood supply (≥ 5 cm in size), they may degenerate [27] [21]. The types of degeneration are hyaline, cystic, myxoid, hemorrhagic, and calcific (Table 2).

Hyaline degeneration is the most common type (60%). Leiomyomas with hyaline degeneration have low signal intensity on T2WI, an appearance similar to that of non-degenerated leiomyomas; however, they enhance to a lesser degree than standard leiomyomas [32] (Figure 4a,b).

Cystic degeneration (4%) is characterized by the presence of cystic areas with high signal intensity on T2-WI that do not enhance [21](Figure 4c,d).

Myxoid degeneration is relatively rare and depends on the presence of gelatinous intralesional foci at gross examination that contain hyaluronic acid–rich mucopolysaccharides [33]. Leiomyomas with myxoid degeneration have an extremely high signal intensity on T2WI and enhance well except for foci of mucinous lakes or clefts. Delayed and prolonged contrast enhancement is due to the presence of myxoid stroma [34](Figure 4e,f).

Hemorrhagic degeneration (red degeneration) is due to hemorrhagic infarction resulting in coagulative necrosis and is associated with pregnancy and oral contraceptives[35]. Red degeneration may also occur after uterine artery embolization (UAE). On MRI, the signal intensity is variable: peripheral or diffuse hyperintensity on T1WI and inhomogeneous signal intensity on T2WI with or without the hypointense rim. The T1-hyperintensity is due to the proteinaceous content of the blood or to the T1-shortening effect of methemoglobin [12] . When the hyperintensity is peripheral, it may be caused by thrombosis of the vessels that surround the lesion [35]. (Figure 4g,h).

Calcific degeneration is associated with end-stage hyaline degeneration and post-UAE treatment changes. On MRI the calcific components produce signal voids on all sequences [10].

Smooth muscle tumor of uncertain malignant potential (STUMP) is a rare heterogeneous tumor that cannot be definitively classified histologically as leiomyoma or leiomyosarcoma[8]. Multiple subtypes have been identified according to nuclear atypia, mitotic rate and necrosis. On MRI, there are no specific features, because STUMP mimics both typical leiomyoma and

leiomyosarcoma. After removal they have a high rate of recurrence (7.3-12.5%) and may recur as low-grade leiomyosarcoma; therefore, long-term follow-up is needed [8,10].

Pitfalls to avoid on MRI:

Distinction between an ovarian mass and a uterine mass: It might be hard to distinguish uterine leiomyoma from a fibrous ovarian mass. In the instance of an ovarian mass, sharp angles between the ovary and the lesion are known as the "beak sign". In contrast, in the case of a uterine mass, a normal ovary will be seen separate from the mass. The "claw sign" (uterine tissue draped around the mass) (Figure 4c) or the "bridging vessels" sign (enlarged and tortuous vessels extending from the uterus to the lesion) suggest the diagnosis of a uterine mass (Figure 4h, 5).

Focal myometrial contractions: Contractions may appear as low T2 signal myometrial masses and may simulate uterine leiomyomas. Since they are transient and usually do not persist during the entire examination they can be easily differentiated from leiomyomas (Figure 6).

Endometrial polyp: Submucosal leiomyoma may be mistaken for an endometrial polyp. Polyps have heterogeneous or high signal on T2WI in contrast to pedunculated submucosal leiomyomas which are low signal on T2WI and have a stalk that arises from the myometrium.

Adenomyomas: (see adenomyosis section below).

Leiomyosarcomas: It is critical to differentiate a benign leiomyoma from leiomyosarcoma. While leiomyosarcomas arise de novo and have no biologic link to leiomyomas [36], they may present with symptoms and imaging features similar to leiomyomas. Large size and rapid growth are unreliable signs of malignancy [36]. Growth of a uterine mass after menopause and elevated LDH, particularly LDH isozyme type 3, is suspicious for leiomyosarcoma [36]. Endometrial sampling may aid diagnosis of uterine sarcoma but sensitivity is limited due to the myometrial origin of the tumor [36,37]. While no single MRI feature can reliably distinguish leiomyosarcomas from atypical leiomyomas, a combination of MRI features may improve the diagnostic performance of MRI for the correct

diagnosis of leiomyosarcoma. In a study from Lakhman et al, the combination of 3 or more of 4 discriminative features including nodular borders, hemorrhage (high-SI on T1WI), T2W dark areas and central areas of nonenhancement were associated with an improved sensitivity and specificity for the diagnosis of leiomyosarcoma[14](Figure 7). Uterine sarcoma also demonstrates rapid early enhancement of the solid components and restricted diffusion[8]. Diffusion restriction alone is insufficient for diagnosis as there is considerable overlap in ADC values between leiomyomas and leiomyosarcoma; leiomyomas may demonstrate restricted diffusion especially cellular leiomyomas[38] (Figure 7). Notably, the presence of restricted diffusion and a T2 blackout effect is highly specific for a leiomyoma[15] (Figure 2). More recently, Thomassin-Naggara et al. reported that using a recursive model combining T2 signal intensity, b1000 images and ADC map with a cut off value 1.23, MRI achieved 92.4% accuracy in distinguishing benign and uncertain or malignant myometrial tumors. The authors concluded that DWI may be of interest to distinguish between uterine sarcomas and benign leiomyomas[31]. Figure 8 is an algorithm to help differentiate leiomyoma and leiomyosarcoma.

Treatment options:

Depending on the spectrum of symptoms a patient is experiencing, they may benefit from conservative management. Asymptomatic leiomyomas do not require treatment. Nonsteroidal anti-inflammatory medications may diminish symptoms of dysmenorrhea, but it is unclear if these effects extend to women with dysmenorrhea because of leiomyomas[39]. Oral contraceptives or gonadotropin-releasing hormone (GnRH) agonists may be used to reduce menstrual bleeding associated with leiomyomas[39,40]. GnRH agonists may also reduce the size of leiomyomas[39]. While some advocate the use of levonorgestrel-releasing intrauterine device (IUD) as a means to reduce menstrual bleeding with leiomyomas, the data to support its effectiveness are limited[39,41]. Since

submucosal leiomyomas increase the risk of IUD expulsion and bleeding complications, they are a relative contraindication for the use of an IUD[40].

Women with refractory abnormal bleeding or those experiencing bulk symptoms, such as pelvic fullness, constipation or urinary symptoms, may be eligible for surgical management. Uterine-sparing myomectomy can be considered for patients with three or fewer dominant symptomatic leiomyomas of less than 8 cm in diameter[40]. Hysteroscopic myomectomy is optimal for the treatment of submucosal leiomyomas that are predominantly intracavitary, are less than 4 cm in size, and have at least 5 mm of intact myometrium overlying the leiomyoma while laparoscopic or open myomectomy is preferred for subserosal or intramural leiomyomas [40]. If the patient no longer desires childbearing, hysterectomy, via abdominal, laparoscopic, or vaginal approach, is a consideration. While there is risk inherent with surgical intervention, hysterectomy yields the highest degree of symptom improvement [42].

Uterine artery embolization (UAE) is a minimally-invasive uterine-sparing treatment option for leiomyomas resulting in abnormal bleeding, anemia, and/or bulk symptoms. UAE is an alternative to myomectomy, but, unlike myomectomy, it is also useful in patients with multiple (>3) and large (> 10 cm) leiomyomas [43]. UAE offers the opportunity to preserve fertility, improves or eliminates bulk symptoms and bleeding, is durable, and has a low complication rate[44,45]. There is a roughly 10-15% treatment failure rate in which patients will require additional treatment with hysterectomy, myomectomy, or repeat UAE[45,46].

Some centers utilize UAE prior to myomectomy. In this scenario, UAE is performed 24-48 hours before standard myomectomy. Compared to myomectomy alone, this combined technique decreases the risk of bleeding requiring transfusion, minimizes the risk of conversion to hysterectomy, and results in a shorter postoperative hospital stay[47].

Adenomyosis:

Epidemiology, clinical symptoms and pathophysiology:

Adenomyosis is a common benign gynecological condition. It is defined as ectopic endometrial glands and stroma in the myometrium more than 2.5 mm from the endometrium-myometrium interface. [5,48]. While it is estimated that up to one-third of patients with adenomyosis are asymptomatic, the symptoms of adenomyosis are common but are nonspecific including dysmenorrhea, menorrhagia, and abnormal vaginal bleeding. Adenomyosis is associated with female infertility possibly in part due to the overlapping pathophysiology and association with endometriosis[52]. The etiology of adenomyosis is still unclear[4]. Exposure to estrogen, prior uterine surgery and parity are known risk factors.

Ultrasound Imaging Features:

Multiple ultrasound features have been associated with adenomyosis including myometrial heterogeneity with thin linear shadowing ("venetian blinds") alternating with increased echogenicity, globular uterine enlargement, asymmetric thickening of the myometrium ("pseudo-widening sign") and isolated or clustered small anechoic cysts [53-62] [63].The ultrasound appearance of adenomyomas may be similar to uterine leiomyoma. Leiomyomas usually have a well-defined border and peripheral color flow, whereas adenomyomas tend to be ill-defined, demonstrate less mass effect and have diffuse and central color flow[59].

MRI imaging features:

MRI is highly accurate for the diagnosis of adenomyosis. In a prospective cohort, Stamatopoulos et al. described a sensitivity of 46.1%, specificity of 99.2%, and positive predictive value of 92.3% of

MRI in the diagnosis of adenomyosis[64]. An MRI classification of adenomyosis was recently proposed by Bazot et al including defining different forms of adenomyosis [65].

Classic MRI appearance of adenomyosis:

- *Subendometrial cysts* is a direct sign of adenomyosis correlated with the presence of endometrial glands within the myometrium. These microcysts typically demonstrate water signal on T1WI and T2WI. Hemorrhagic content may accumulate within the cysts and demonstrate T1 hyperintense signal[4]. They are mainly located in the superficial myometrium and are highly specific (98%). However, they are only detected in 50% of cases[66-70] (Figure 9).
- *Thickening of the junctional zone (JZ)* is an indirect sign related to myometrial hypertrophy, secondary to the presence of ectopic endometrial glands within the myometrium. A JZ thickness of greater than 12 mm has a diagnostic accuracy of 85%, specificity of 96%, and sensitivity of 63% to predict adenomyosis[67]. The *JZ differential sign* was described by Dueholm and al as the difference between maximal and minimal thicknesses in the anterior and posterior uterine JZ; a differential of greater than 5 mm may be a more reliable marker than a JZ thickness of greater than 12 mm[71] (Figure 9).
- Because adenomyosis may demonstrate variable degrees of enhancement, intravenous contrast does not enhance the diagnostic capacity of MRI.

Subtypes of adenomyosis:

- *Adenomyoma* is a mass-like confluence of ectopic endometrial glands within the myometrium, distinct from the JZ. The distinction from leiomyoma may be challenging; adenomyomas are usually ill-defined low signal T2W mass which may contain punctate foci of high T2 signal[7,69,72,73] (Figure 10).

- *Hemorrhagic cystic adenomyosis (adenomyotic cyst)* is a rare subtype of adenomyosis and is frequently symptomatic with dysmenorrhea and menorrhagia. This lesion develops following spontaneous hemorrhage of ectopic endometrial glands[74]. The hemorrhage is contained by a partial or complete rim of myometrial tissue, resulting in a cyst- like appearance with high signal on T1WI and a low signal rim on T2WI. The cyst may be submucosal, intramural, or subserosal[74,75](Figure 11).
- *External adenomyosis* arises in the outer part of the uterus, most likely in the posterior myometrium disrupting the serosa but not affecting the JZ. It is usually associated with deep endometriosis. On MRI, it appears as an ill-defined subserosal posterior T2 hypointense mass/pseudomass and may contains T2 hyperintense small cystic areas.
- *Adenomyomatous polyp or polypoid adenomyoma* presents as a polypoid mass in the lower uterine endometrium or endocervix, and accounts for about 2% of all endometrial polyps. On MRI, it is a hypointense polypoid mass associated with T2WI hyperintense foci[76-78].

MRI Differential diagnosis:

- *Cyclic Physiologic Changes of the Uterus (Pseudo-thickening of the JZ*): thickness of the junctional zone is hormone-dependent and changes according to the menstrual cycle. Preferably, MRI should be not performed during menstruation to avoid this pitfall[72,75].
- *Non-measurable junctional zone:* the JZ may not be measurable in postmenopausal patients and in women using contraceptive drugs[2,9,79-84].
- *Myometrial contractions*: transient uterine contractions are hypointense T2W bands perpendicular to the JZ or focal thickening of the JZ and can mimic focal adenomyosis[85]. Repeating the acquisition of images within a few minutes may demonstrate their transient nature; Cine MRI may also help (Figure 6).

- *Endometrial cancer:* adenomyosis can be seen in 20% of patients with endometrial cancer[3]. Evaluation of myometrial invasion may become difficult with the coexistence of adenomyosis as it may be responsible for a pseudo widening of the endometrium confused as myometrial invasion[3,86-88] (Figure 12). Since endometrial cancer can frequently extend into the ectopic endometrial tissue in adenomyosis, the true degree of myometrial invasion may be difficult to evaluate in the setting of concomitant adenomyosis. DWI may help to define the depth of myometrial invasion; adenomyosis does not restrict diffusion whereas endometrial cancer does[89] (Figure 13).
- *Leiomyoma:* traditionally, adenomyomas present as a T2 hypointense mass with ill-defined borders, minimal mass effect and with multiple bright foci. In contrast, leiomyoma, besides being also T2 hypointense, also have a well-defined border, adjacent mass effect, and large vessels surrounding the lesion[90] (Figure 10).

Treatment options:

Medical therapy for adenomyosis relies upon hormonal suppression. Oral contraceptives and GnRH agonists both induce amenorrhea and thus reduce symptoms of pain and bleeding. Symptoms tend to recur with cessation of therapy91. Levonorgestrel-releasing IUDs may be slightly more efficacious than oral contraceptives in reducing pain and uterine bleeding92 and appear to improve quality of life measures similarly to slightly more than hysterectomy93. Traditionally, the standard treatment for symptomatic adenomyosis had been hysterectomy91. However, uterine-sparing techniques, including either complete or partial adenomyomectomy via open or laparoscopic approaches, can be considered in women wishing to maintain fertility, those who cannot tolerate a large operation, or in those wishing to consider a more conservative approach. Complete adenomyomectomy is effective in the setting of a focal adenomyoma.

Partial adenomyomectomy, removal of a portion of the clinically recognizable adenomyosis, is employed in the setting of diffuse adenomyosis when complete resection would effectively result in a "functional hysterectomy." All of the uterine-sparing operative techniques yield improvements in pain in 82-85% of patients, reduction in abnormal uterine bleeding in 50-69% of patients and preserve fertility in 43-47%[94].

In select patients, UAE can be used to treat adenomyosis with or without leiomyomas. Symptom relief may not be as great or as durable as expected in the setting of isolated leiomyomas[95] and patients with combined adenomyosis and leiomyomas tend to experience greater symptom relief from UAE than patients with pure adenomyosis [96,97]. Ultimately, with UAE, hysterectomy can be avoided in up to 85% of patients with symptomatic adenomyosis [96,97].

Conclusion

Benign uterine diseases, including adenomyosis and leiomyomas, are common conditions affecting women of all ages. Ultrasound is often the initial imaging study obtained; however, MRI is the preferred modality for additional lesion characterization and provides critical information to assist in selecting the appropriate therapies for symptomatic patients. Treatment options for adenomyosis and leiomyomas include medical, surgical, and minimally invasive techniques such as uterine artery embolization.

TABLE 1 Protocol

T2 WI	High-resolution T2 sequences in the axial, oblique, sagittal, and coronal planes. The axial oblique T2W sequence perpendicular to the corpus of the uterus is particularly useful to evaluate the location of the lesion relative to the endometrial cavity.
T1 WI	Axial T1W sequence of the pelvis with and without fat suppression. Axial T1W sequence is useful to evaluate the presence of fat or blood contents and can be used to detect the presence of lymph nodes and bone marrow abnormalities.
Large FOV T1/T2WI	Large FOV T1 or T2W sequence of the upper abdomen. It allows visualization of secondary signs of pelvic mass effect such as hydronephrosis and malignant disease such as lymph nodes or peritoneal carcinomatosis.
Contrast-enhanced T1WI	Contrast-enhanced axial T1-weighted images (T1WI) of the pelvis with fat saturation. It allows further lesion characterization, vascularization and its differentiation from an adnexal mass.
Dynamic contrast injection/MR angiography	Dynamic contrast injection/MR angiography is recommended if uterine artery embolization may be a possibility in order to evaluate uterine artery anatomy and collateral gonadal arterial supply.
DWI	DWI is not mandatory but has shown added value for lesion characterization and distinction between leiomyoma and leiomyosarcoma.

TABLE 2

MRI features of leiomyomas and leiomyosarcomas.

	T2WI Signal	T2WI Border	T1WI	C+	DWI/ADC
Type of Leiomyoma					
Non-degenerated	Hypointense	Well-defined	Isointense	Variable	Hypointense
Cellular subtype	Hyperintense	Well-defined	Isointense	Vivid Enhancement	Hyperintense
Lipoleiomyoma subtype	Variable - Fat component (hyperintense)	Well-defined	Variable - Fat component (hyperintense)	Variable	Hypointense
Degeneration Type					
Hyaline	Hypointense	Well-defined	Isointense	Moderate enhancement	Hypointense
Cystic	Hyperintense	Well-defined	Hypointense	No enhancement	Hypointense
Myxoid	Very hyperintense	Well-defined	Hypointense	Delayed enhancement	Hypointense
Hemorrhagic	Variable	Well-defined	Hyperintense	Variable	Hypointense
Calcific	HypoT2	Well-defined	Hypointense	No enhancement	Hypointense
Leiomyosarcoma	T2 Dark areas	Nodular border	Presence of High T1-SI related to blood	Enhancement with central necrosis	High DWI/Low ADC

Legends

Figure 1: Leiomyoma FIGO classification system according to location. **(a)** Drawing depicts the leiomyoma FIGO classification, as FIGO 0: pedunculated intracavitary; FIGO 1: submucosal <50% intramural; FIGO 2: submucosal ≥ 50% intramural; FIGO 3: contacts endometrium, 100%

intramural; FIGO 4: intramural; FIGO 5: subserosal ≥ 50% intramural; FIGO 6: subserosal <50 % intramural; FIGO 7: subserosal pedunculated; FIGO 8: other (specify e.g. cervical, parasitic). **(b)** Sagittal and **(c)** axial T2-weighted images show multiple leiomyomas in different locations, each labelled with their MRI FIGO classification.

Figure 2: Typical leiomyoma. **(a)** Sagittal and **(b)** axial T2-weighted images, **(c)** axial T1-weighted image, **(d)** axial DW image with **(e)** corresponding ADC map, and **(f)** gadolinium-enhanced axial T1-weighted fat saturated images show a myometrial lesion with endometrial contact (arrow) in keeping with a FIGO 3 leiomyoma. Non-degenerated leiomyoma appears as a well-defined lesion with hypointense signal intensity on T2-weighted images related to the outer myometrium **(a-b)**, isointense signal intensity on T1-weighted image **(c)** and homogeneous contrast-enhancement **(f)**. The "blackout phenomenon" is illustrated with no signs of restricted diffusion with low signal intensity on DW image (b=1000) **(d)** and corresponding ADC map **(e**.

Figure 3: Cellular leiomyoma. **(a)** Sagittal and **(b)** axial T2-weighted images show a well-delineated lesion (arrow) of intermediate to high signal intensity without T2 dark areas. **(c)** Axial oblique T1-weighted image show isointense lesion without hemorrhage (arrow). **(d)** Axial oblique DW image (b=1000) show high signal intensity (arrow) with restriction on **(e)** corresponding ADC map (arrow). **(f)** Contrast-enhanced axial oblique T1-weighted fat saturated image shows avid and heterogeneous enhancement without necrosis (arrow). The absence of hemorrhage and necrosis, T2 dark signal, and the presence of well-defined border favor a cellular leiomyoma over leiomyosarcoma; this was confirmed histologically.

Figure 4: Different types of leiomyoma degeneration**. Hyaline degeneration. (a)** Axial T2-weighted image and **(b)** contrast-enhanced axial T1-weighted fat saturated image show a leiomyoma (arrow) with hypointense signal intensity on T2-weighted image and poor enhancement after gadolinium injection, suggesting hyaline degeneration. **Cystic degeneration. (c)** Axial T2-weighted image and **(d)** sagittal T2-weighted image show a large well-defined cystic lesion (arrow) with high T2 signal intensity, consistent with cystic leiomyoma due to its uterine origin (claw sign). **Myxoid degeneration. (e)** Sagittal T2-weighted fat saturated image and **(f)** contrast-enhanced sagittal T1-weighted fat saturated image show a leiomyoma (arrow) presenting areas with high signal intensity on T2-weighted image and enhancement after gadolinium injection, with the exception of the non-enhancing mucinous lakes, suggesting a myxoid leiomyoma. **Hemorrhagic degeneration. (g)** Axial T1-weighted fat saturated image and **(h)** axial T2-weighted fat saturated image show a left para-uterine lesion (white arrow) with a component of very high signal intensity on T1-weighted image and low signal intensity on T2-weighted image, suggesting intralesional hemorrhage. The lesion is a hemorrhagic subserosal pedunculated leiomyoma (MRI FIGO 7) with enlarged and tortuous vessel (black arrow, h) that extend from the uterus to the mass (bridging vessel sign), indicating the uterine origin of the lesion.

Figure 5: Indeterminate origin of a mass: ovarian versus uterine. Axial T2-weighted image shows a well-defined left para-uterine mass with low signal intensity that could resemble either a uterine leiomyoma or ovarian fibroma. In this case, the left ovary (black arrow) is normal and separate from the mass. Enlarged and tortuous vessels extended from the uterus to supply the mass (white arrows, bridging vessels sign), suggesting the diagnosis of uterine leiomyoma.

Figure 6: Transient myometrial contraction. **(a)** Sagittal and **(b)** axial T2-weighted fat saturated images. Axial T2-weighted image shows hypointense bands perpendicular to the junctional zone in the anterior myometrium (arrows, **b**). This finding was absent on previous sagittal T2-weighted image that shows normal uterus with thin and distinct junctional zone (arrow, **a**), confirming the diagnosis of transient myometrial contraction.

Figure 7: Leiomyosarcoma. **(a)** axial T2-weighted images, **(b)** axial T1-weighted image, **(c)** axial DW image and **(d)** gadolinium-enhanced axial T1-weighted fat saturated image. Axial T2-weighted image shows dark T2 area (arrows, **a**) and ill-defined border. Hemorrhage is seen on the axial T1-weighted image (arrows, **b**). **(c)** Axial oblique DW image (b=1000) show high signal intensity (arrow). **(d)** Contrast-enhanced axial oblique T1-weighted fat saturated image shows heterogeneous enhancement with central necrosis (arrow). Those combined features are suggestive of leiomyosarcoma which was confirmed histologically.

Figure 8: Flow chart describing the role of MRI in differentiating leiomyoma and uterine sarcoma.

Figure 9: Adenomyosis. **(a)** Drawing shows classic features of adenomyosis: subendometrial cysts and diffuse thickening (orange arrow) of the junctional zone (JZ). **(b)** Sagittal T2-weighted image shows an enlarged uterus with the classic MRI appearance of adenomyosis, as thickening of the JZ particularly of the anterior myometrium (orange arrow) with multiple high T2 signal foci (white arrows). **(c)** Axial T2-weighted image and **(d)** axial T1-weighted fat saturated image show a high T2 and high T1 focus within the anterior myometrium (arrow, **c-d**) due to hemorrhagic content.

Figure 10: Adenomyoma. **(a)** Drawing shows the different features of adenomyoma and leiomyoma. An adenomyoma is T2 dark with internal bright foci due to endometrial glands, while a typical leiomyoma is homogeneously dark with a bright peripheral rim due to perilesional edema that generally causes more adjacent mass effect than adenomyoma. **(b)** Sagittal and **(c)** axial T2-weighted images show an ill-defined, low signal intensity mass with embedded hyperintense foci in the posterior myometrium (arrow, **b**) suggesting an adenomyoma. **(c)** Axial oblique T2-weighted images show a well-defined, low signal intensity mass with embedded hyperintense foci bulging into the endometrium (arrow, **c**) suggesting a subendometrial adenomyoma. **(d)** Sagittal T2-weighted image shows an enlarged uterus with the coexistence of an adenomyoma, as ill-defined hypointense mass-like lesion with embedded hyperintense punctate foci in the posterior myometrium (white arrow), and a leiomyoma, as well-defined very hypointense mass in the anterior myometrium causing adjacent mass effect (black arrow).

Figure 11: Hemorrhagic cystic adenomyosis. **(a)** Sagittal T2-weighted fat saturated image shows diffuse thickening of the JZ and a single intramural focus of high signal intensity in the anterior myometrium (arrow). **(b-c)** The cyst-like focus is better seen on **(b)** axial T1-weighted image and **(c)** axial T2-weighted image characterized by T1 and T2 high signal (arrow, **b-c**), confirming hemorrhagic content.

Figure 12: Pseudowidening of the JZ with coexisting endometrial cancer. **(a)** Drawing showing the pseudowidening of the JZ. Sagittal **(b)** and **(c)** axial oblique T2-weighted image shows an intermediate T2 signal within the endometrial cavity (orange arrow) with diffuse thickening of the JZ bulging in the endometrial cavity (pseudowidening of the JZ, black arrow). Note the large cystic

area on **b** consistent with a subendometrial cyst. On fused T2-DWI image **(d)** signal hyperintensity is solely seen at the level of the intermediate T2 signal corresponding to the endometrial cancer (orange arrow). No areas of restricted diffusion are seen within the pseudowidening of the JZ. In this case, DWI was particularly helpful to delineate the cancer.

Figure 13: Endometrial cancer with coexisting adenomyosis in 3 differents patients (a-b,c-d,e-f). Axial oblique T2-weighted image **(a ,c)** shows an intermediate T2 signal within the endometrial cavity (orange arrow) with a diffuse thickening of the JZ and a subendometrial cyst (white arrow). The Subendometrial cyst in **c** demonstrates the same signal as the endometrial thickening which is confirmed on DWI **(b,d)**. In the first case (figure 12), the endometrial cancer does not extend into the adenomyosis; in this case (figure 13), tumor extends into the adenomyosis. DWI was again particularly helpful to delineate the cancer. **(e)** Axial oblique T2-weighted image shows an intermediate T2 signal within the endometrial cavity and within the myometrium (very ill-defined) (orange arrow) with diffuse thickening of the JZ (white arrow). **(f)** DWI shows a large very well-defined area of hyperintense signal consistent with an endometrial cancer with deep myometrial invasion (orange arrow); again DWI was helpful to differentiate the tumor from the thickening of the JZ.

1. American Association of Gynecologic Laparoscopists : Advancing Minimally Invasive Gynecology W. AAGL practice report: practice guidelines for the diagnosis and management of submucous leiomyomas. *J Minim Invasive Gynecol.* 2012;19(2):152-171.
2. Brosens JJ, de Souza NM, Barker FG. Uterine junctional zone: function and disease. *Lancet.* 1995;346(8974):558-560.
3. Habiba M, Pluchino N, Petignat P, Bianchi P, Brosens IA, Benagiano G. Adenomyosis and Endometrial Cancer: Literature Review. *Gynecol Obstet Invest.* 2018;83(4):313-328.
4. Krentel H, Cezar C, Becker S, et al. From Clinical Symptoms to MR Imaging: Diagnostic Steps in Adenomyosis. *Biomed Res Int.* 2017;2017:1514029.
5. Munro MG. Uterine polyps, adenomyosis, leiomyomas, and endometrial receptivity. *Fertil Steril.* 2019;111(4):629-640.
6. Vannuccini S, Petraglia F. Recent advances in understanding and managing adenomyosis. *F1000Res.* 2019;8.
7. Agostinho L, Cruz R, Osorio F, Alves J, Setubal A, Guerra A. MRI for adenomyosis: a pictorial review. *Insights Imaging.* 2017;8(6):549-556.
8. Bolan C, Caserta MP. MR imaging of atypical fibroids. *Abdom Radiol (NY).* 2016;41(12):2332-2349.
9. Brown HK, Stoll BS, Nicosia SV, et al. Uterine junctional zone: correlation between histologic findings and MR imaging. *Radiology.* 1991;179(2):409-413.
10. DeMulder D, Ascher SM. Uterine Leiomyosarcoma: Can MRI Differentiate Leiomyosarcoma From Benign Leiomyoma Before Treatment? *AJR Am J Roentgenol.* 2018;211(6):1405-1415.
11. Deshmukh SP, Gonsalves CF, Guglielmo FF, Mitchell DG. Role of MR imaging of uterine leiomyomas before and after embolization. *Radiographics.* 2012;32(6):E251-281.
12. Dudiak CM, Turner DA, Patel SK, Archie JT, Silver B, Norusis M. Uterine leiomyomas in the infertile patient: preoperative localization with MR imaging versus US and hysterosalpingography. *Radiology.* 1988;167(3):627-630.
13. Kubik-Huch RA, Weston M, Nougaret S, et al. European Society of Urogenital Radiology (ESUR) Guidelines: MR Imaging of Leiomyomas. *Eur Radiol.* 2018;28(8):3125-3137.
14. Lakhman Y, Veeraraghavan H, Chaim J, et al. Differentiation of Uterine Leiomyosarcoma from Atypical Leiomyoma: Diagnostic Accuracy of Qualitative MR Imaging Features and Feasibility of Texture Analysis. *Eur Radiol.* 2017;27(7):2903-2915.
15. Sato K, Yuasa N, Fujita M, Fukushima Y. Clinical application of diffusion-weighted imaging for preoperative differentiation between uterine leiomyoma and leiomyosarcoma. *Am J Obstet Gynecol.* 2014;210(4):368 e361-368 e368.
16. Dubuisson J. The current place of mini-invasive surgery in uterine leiomyoma management. *J Gynecol Obstet Hum Reprod.* 2019;48(2):77-81.
17. Lewis TD, Malik M, Britten J, San Pablo AM, Catherino WH. A Comprehensive Review of the Pharmacologic Management of Uterine Leiomyoma. *Biomed Res Int.* 2018;2018:2414609.
18. Owen C, Armstrong AY. Clinical management of leiomyoma. *Obstet Gynecol Clin North Am.* 2015;42(1):67-85.
19. Stokes LS, Wallace MJ, Godwin RB, Kundu S, Cardella JF, Society of Interventional Radiology Standards of Practice C. Quality improvement guidelines for uterine artery embolization for symptomatic leiomyomas. *J Vasc Interv Radiol.* 2010;21(8):1153-1163.
20. Burke CT, Funaki BS, Ray CE, Jr., et al. ACR Appropriateness Criteria(R) on treatment of uterine leiomyomas. *J Am Coll Radiol.* 2011;8(4):228-234.

21. Murase E, Siegelman ES, Outwater EK, Perez-Jaffe LA, Tureck RW. Uterine leiomyomas: histopathologic features, MR imaging findings, differential diagnosis, and treatment. *Radiographics.* 1999;19(5):1179-1197.
22. Munro MG, Critchley HO, Broder MS, Fraser IS, Disorders FWGoM. FIGO classification system (PALM-COEIN) for causes of abnormal uterine bleeding in nongravid women of reproductive age. *Int J Gynaecol Obstet.* 2011;113(1):3-13.
23. Araki H, Yoshizako T, Yoshida R, Maruyama M, Ishikawa N, Kitagaki H. MR Imaging of Parasitic Leiomyoma with Red Degeneration. *Magn Reson Med Sci.* 2019.
24. Garrido Oyarzun MF, Saco A, Castelo-Branco C. Anterior abdominal wall parasitic leiomyoma: case report. *Gynecol Endocrinol.* 2018;34(2):103-106.
25. Fasih N, Prasad Shanbhogue AK, Macdonald DB, et al. Leiomyomas beyond the uterus: unusual locations, rare manifestations. *Radiographics.* 2008;28(7):1931-1948.
26. Van den Bosch T, Dueholm M, Leone FP, et al. Terms, definitions and measurements to describe sonographic features of myometrium and uterine masses: a consensus opinion from the Morphological Uterus Sonographic Assessment (MUSA) group. *Ultrasound Obstet Gynecol.* 2015;46(3):284-298.
27. Hricak H, Tscholakoff D, Heinrichs L, et al. Uterine leiomyomas: correlation of MR, histopathologic findings, and symptoms. *Radiology.* 1986;158(2):385-391.
28. Dueholm M, Lundorf E, Hansen ES, Ledertoug S, Olesen F. Accuracy of magnetic resonance imaging and transvaginal ultrasonography in the diagnosis, mapping, and measurement of uterine myomas. *Am J Obstet Gynecol.* 2002;186(3):409-415.
29. Mittl RL, Jr., Yeh IT, Kressel HY. High-signal-intensity rim surrounding uterine leiomyomas on MR images: pathologic correlation. *Radiology.* 1991;180(1):81-83.
30. Nougaret S, Horta M, Sala E, et al. Endometrial Cancer MRI staging: Updated Guidelines of the European Society of Urogenital Radiology. *Eur Radiol.* 2019;29(2):792-805.
31. Thomassin-Naggara I, Dechoux S, Bonneau C, et al. How to differentiate benign from malignant myometrial tumours using MR imaging. *Eur Radiol.* 2013;23(8):2306-2314.
32. Arleo EK, Schwartz PE, Hui P, McCarthy S. Review of Leiomyoma Variants. *AJR Am J Roentgenol.* 2015;205(4):912-921.
33. Prayson RA, Hart WR. Pathologic considerations of uterine smooth muscle tumors. *Obstet Gynecol Clin North Am.* 1995;22(4):637-657.
34. Ueda H, Togashi K, Konishi I, et al. Unusual appearances of uterine leiomyomas: MR imaging findings and their histopathologic backgrounds. *Radiographics.* 1999;19 Spec No:S131-145.
35. Kawakami S, Togashi K, Konishi I, et al. Red degeneration of uterine leiomyoma: MR appearance. *J Comput Assist Tomogr.* 1994;18(6):925-928.
36. Ricci S, Stone RL, Fader AN. Uterine leiomyosarcoma: Epidemiology, contemporary treatment strategies and the impact of uterine morcellation. *Gynecologic oncology.* 2017;145(1):208-216.
37. Rieber A, Aschoff A, Nussle K, et al. MRI in the diagnosis of small bowel disease: use of positive and negative oral contrast media in combination with enteroclysis. *Eur Radiol.* 2000;10(9):1377-1382.
38. Namimoto T, Yamashita Y, Awai K, et al. Combined use of T2-weighted and diffusion-weighted 3-T MR imaging for differentiating uterine sarcomas from benign leiomyomas. *Eur Radiol.* 2009;19(11):2756-2764.
39. American College of O, Gynecologists. ACOG practice bulletin. Alternatives to hysterectomy in the management of leiomyomas. *Obstet Gynecol.* 2008;112(2 Pt 1):387-400.

40. Marret H, Fritel X, Ouldamer L, et al. Therapeutic management of uterine fibroid tumors: updated French guidelines. *Eur J Obstet Gynecol Reprod Biol.* 2012;165(2):156-164.
41. Sangkomkamhang US, Lumbiganon P, Laopaiboon M, Mol BW. Progestogens or progestogen-releasing intrauterine systems for uterine fibroids. *Cochrane Database Syst Rev.* 2013(2):CD008994.
42. Spies JB, Bradley LD, Guido R, Maxwell GL, Levine BA, Coyne K. Outcomes from leiomyoma therapies: comparison with normal controls. *Obstet Gynecol.* 2010;116(3):641-652.
43. Smeets AJ, Nijenhuis RJ, van Rooij WJ, et al. Uterine artery embolization in patients with a large fibroid burden: long-term clinical and MR follow-up. *Cardiovasc Intervent Radiol.* 2010;33(5):943-948.
44. Lohle PN, Voogt MJ, De Vries J, et al. Long-term outcome of uterine artery embolization for symptomatic uterine leiomyomas. *J Vasc Interv Radiol.* 2008;19(3):319-326.
45. Goodwin SC, Spies JB, Worthington-Kirsch R, et al. Uterine artery embolization for treatment of leiomyomata: long-term outcomes from the FIBROID Registry. *Obstet Gynecol.* 2008;111(1):22-33.
46. Pelage JP, Cazejust J, Pluot E, et al. Uterine fibroid vascularization and clinical relevance to uterine fibroid embolization. *Radiographics.* 2005;25 Suppl 1:S99-117.
47. McLucas B, Voorhees WD, 3rd. The effectiveness of combined abdominal myomectomy and uterine artery embolization. *Int J Gynaecol Obstet.* 2015;130(3):241-243.
48. Tetikkurt S, Celik E, Tas H, Cay T, Isik S, Usta AT. Coexistence of adenomyosis, adenocarcinoma, endometrial and myometrial lesions in resected uterine specimens. *Mol Clin Oncol.* 2018;9(2):231-237.
49. Vercellini P, Parazzini F, Oldani S, Panazza S, Bramante T, Crosignani PG. Adenomyosis at hysterectomy: a study on frequency distribution and patient characteristics. *Hum Reprod.* 1995;10(5):1160-1162.
50. Vavilis D, Agorastos T, Tzafetas J, et al. Adenomyosis at hysterectomy: prevalence and relationship to operative findings and reproductive and menstrual factors. *Clin Exp Obstet Gynecol.* 1997;24(1):36-38.
51. Weiss G, Maseelall P, Schott LL, Brockwell SE, Schocken M, Johnston JM. Adenomyosis a variant, not a disease? Evidence from hysterectomized menopausal women in the Study of Women's Health Across the Nation (SWAN). *Fertil Steril.* 2009;91(1):201-206.
52. Tskhay VB, Schindler AE, Mikailly GT. Diffuse massive adenomyosis and infertility. Is it possible to treat this condition? *Horm Mol Biol Clin Investig.* 2019;37(1).
53. Andres MP, Borrelli GM, Ribeiro J, Baracat EC, Abrao MS, Kho RM. Transvaginal Ultrasound for the Diagnosis of Adenomyosis: Systematic Review and Meta-Analysis. *J Minim Invasive Gynecol.* 2018;25(2):257-264.
54. Atzori E, Tronci C, Sionis L. Transvaginal ultrasound in the diagnosis of diffuse adenomyosis. *Gynecol Obstet Invest.* 1996;42(1):39-41.
55. Dueholm M. Transvaginal ultrasound for diagnosis of adenomyosis: a review. *Best Pract Res Clin Obstet Gynaecol.* 2006;20(4):569-582.
56. Dueholm M, Lundorf E. Transvaginal ultrasound or MRI for diagnosis of adenomyosis. *Curr Opin Obstet Gynecol.* 2007;19(6):505-512.
57. Hanafi M. Ultrasound diagnosis of adenomyosis, leiomyoma, or combined with histopathological correlation. *J Hum Reprod Sci.* 2013;6(3):189-193.
58. Konrad J, Merck D, Wu JY, Tuomi A, Beland M. Improving Ultrasound Detection of Uterine Adenomyosis Through Computational Texture Analysis. *Ultrasound Q.* 2018;34(1):29-31.

59. Sharma K, Bora MK, Venkatesh BP, et al. Role of 3D Ultrasound and Doppler in Differentiating Clinically Suspected Cases of Leiomyoma and Adenomyosis of Uterus. *J Clin Diagn Res.* 2015;9(4):QC08-12.
60. Van den Bosch T, Van Schoubroeck D. Ultrasound diagnosis of endometriosis and adenomyosis: State of the art. *Best Pract Res Clin Obstet Gynaecol.* 2018;51:16-24.
61. Atri M, Reinhold C, Mehio AR, Chapman WB, Bret PM. Adenomyosis: US features with histologic correlation in an in-vitro study. *Radiology.* 2000;215(3):783-790.
62. Van den Bosch T, de Bruijn AM, de Leeuw RA, et al. Sonographic classification and reporting system for diagnosing adenomyosis. *Ultrasound Obstet Gynecol.* 2019;53(5):576-582.
63. Cunningham RK, Horrow MM, Smith RJ, Springer J. Adenomyosis: A Sonographic Diagnosis. *Radiographics.* 2018;38(5):1576-1589.
64. Stamatopoulos CP, Mikos T, Grimbizis GF, et al. Value of magnetic resonance imaging in diagnosis of adenomyosis and myomas of the uterus. *J Minim Invasive Gynecol.* 2012;19(5):620-626.
65. Bazot M, Darai E. Role of transvaginal sonography and magnetic resonance imaging in the diagnosis of uterine adenomyosis. *Fertil Steril.* 2018;109(3):389-397.
66. Reinhold C, Atri M, Mehio A, Zakarian R, Aldis AE, Bret PM. Diffuse uterine adenomyosis: morphologic criteria and diagnostic accuracy of endovaginal sonography. *Radiology.* 1995;197(3):609-614.
67. Reinhold C, McCarthy S, Bret PM, et al. Diffuse adenomyosis: comparison of endovaginal US and MR imaging with histopathologic correlation. *Radiology.* 1996;199(1):151-158.
68. Reinhold C, Tafazoli F, Mehio A, et al. Uterine adenomyosis: endovaginal US and MR imaging features with histopathologic correlation. *Radiographics.* 1999;19 Spec No:S147-160.
69. Reinhold C, Tafazoli F, Wang L. Imaging features of adenomyosis. *Hum Reprod Update.* 1998;4(4):337-349.
70. Tafazoli F, Reinhold C. Uterine adenomyosis: current concepts in imaging. *Semin Ultrasound CT MR.* 1999;20(4):267-277.
71. Dueholm M, Lundorf E, Hansen ES, Sorensen JS, Ledertoug S, Olesen F. Magnetic resonance imaging and transvaginal ultrasonography for the diagnosis of adenomyosis. *Fertil Steril.* 2001;76(3):588-594.
72. Tamai K, Togashi K, Ito T, Morisawa N, Fujiwara T, Koyama T. MR imaging findings of adenomyosis: correlation with histopathologic features and diagnostic pitfalls. *Radiographics.* 2005;25(1):21-40.
73. Novellas S, Chassang M, Delotte J, et al. MRI characteristics of the uterine junctional zone: from normal to the diagnosis of adenomyosis. *AJR Am J Roentgenol.* 2011;196(5):1206-1213.
74. Troiano RN, Flynn SD, McCarthy S. Cystic adenomyosis of the uterus: MRI. *J Magn Reson Imaging.* 1998;8(6):1198-1202.
75. Takeuchi M, Matsuzaki K. Adenomyosis: usual and unusual imaging manifestations, pitfalls, and problem-solving MR imaging techniques. *Radiographics.* 2011;31(1):99-115.
76. Takeuchi M, Matsuzaki K, Harada M. MR manifestations of uterine polypoid adenomyoma. *Abdom Imaging.* 2015;40(3):480-487.
77. Patel N, Hatfield J, Sohaey R, Coakley FV. MRI of prolapsed polypoid adenomyoma: Expanding the differential diagnosis for the broccoli sign. *Clin Imaging.* 2018;52:177-179.
78. Sajjad N, Iqbal H, Khandwala K, Afzal S. Polypoid Adenomyoma of the Uterus. *Cureus.* 2019;11(2):e4044.

79. McCarthy S, Scott G, Majumdar S, et al. Uterine junctional zone: MR study of water content and relaxation properties. *Radiology.* 1989;171(1):241-243.
80. Scoutt LM, Flynn SD, Luthringer DJ, McCauley TR, McCarthy SM. Junctional zone of the uterus: correlation of MR imaging and histologic examination of hysterectomy specimens. *Radiology.* 1991;179(2):403-407.
81. Masui T, Katayama M, Kobayashi S, et al. Changes in myometrial and junctional zone thickness and signal intensity: demonstration with kinematic T2-weighted MR imaging. *Radiology.* 2001;221(1):75-85.
82. Lesny P, Killick SR. The junctional zone of the uterus and its contractions. *BJOG.* 2004;111(11):1182-1189.
83. Fusi L, Cloke B, Brosens JJ. The uterine junctional zone. *Best Pract Res Clin Obstet Gynaecol.* 2006;20(4):479-491.
84. Kiguchi K, Kido A, Kataoka M, et al. Uterine peristalsis and junctional zone: correlation with age and postmenopausal status. *Acta Radiol.* 2017;58(2):224-231.
85. Ozsarlak O, Schepens E, de Schepper AM, Deckers F, Parizel PM, Campo R. Transient uterine contraction mimicking adenomyosis on MRI. *Eur Radiol.* 1998;8(1):54-56.
86. Hertlein L, Rath J, Zeder-Goss C, et al. Coexistence of adenomyosis uteri and endometrial cancer is associated with an improved prognosis compared with endometrial cancer only. *Oncol Lett.* 2017;14(3):3302-3308.
87. Aydin HA, Toptas T, Bozkurt S, Pestereli E, Simsek T. Impact of coexistent adenomyosis on outcomes of patients with endometrioid endometrial cancer: a propensity score-matched analysis. *Tumori.* 2018;104(1):60-65.
88. Erkilinc S, Taylan E, Gulseren V, et al. The Effect of Adenomyosis in Myometrial Invasion and Overall Survival in Endometrial Cancer. *Int J Gynecol Cancer.* 2018;28(1):145-151.
89. Jha RC, Zanello PA, Ascher SM, Rajan S. Diffusion-weighted imaging (DWI) of adenomyosis and fibroids of the uterus. *Abdom Imaging.* 2014;39(3):562-569.
90. Mark AS, Hricak H, Heinrichs LW, et al. Adenomyosis and leiomyoma: differential diagnosis with MR imaging. *Radiology.* 1987;163(2):527-529.
91. Garcia L, Isaacson K. Adenomyosis: review of the literature. *J Minim Invasive Gynecol.* 2011;18(4):428-437.
92. Shaaban OM, Ali MK, Sabra AM, Abd El Aal DE. Levonorgestrel-releasing intrauterine system versus a low-dose combined oral contraceptive for treatment of adenomyotic uteri: a randomized clinical trial. *Contraception.* 2015;92(4):301-307.
93. Ozdegirmenci O, Kayikcioglu F, Akgul MA, et al. Comparison of levonorgestrel intrauterine system versus hysterectomy on efficacy and quality of life in patients with adenomyosis. *Fertil Steril.* 2011;95(2):497-502.
94. Grimbizis GF, Mikos T, Tarlatzis B. Uterus-sparing operative treatment for adenomyosis. *Fertil Steril.* 2014;101(2):472-487.
95. Froeling V, Scheurig-Muenkler C, Hamm B, Kroencke TJ. Uterine artery embolization to treat uterine adenomyosis with or without uterine leiomyomata: results of symptom control and health-related quality of life 40 months after treatment. *Cardiovasc Intervent Radiol.* 2012;35(3):523-529.
96. de Bruijn AM, Smink M, Hehenkamp WJK, et al. Uterine Artery Embolization for Symptomatic Adenomyosis: 7-Year Clinical Follow-up Using UFS-Qol Questionnaire. *Cardiovasc Intervent Radiol.* 2017;40(9):1344-1350.
97. de Bruijn AM, Smink M, Lohle PNM, et al. Uterine Artery Embolization for the Treatment of Adenomyosis: A Systematic Review and Meta-Analysis. *J Vasc Interv Radiol.* 2017;28(12):1629-1642 e1621.

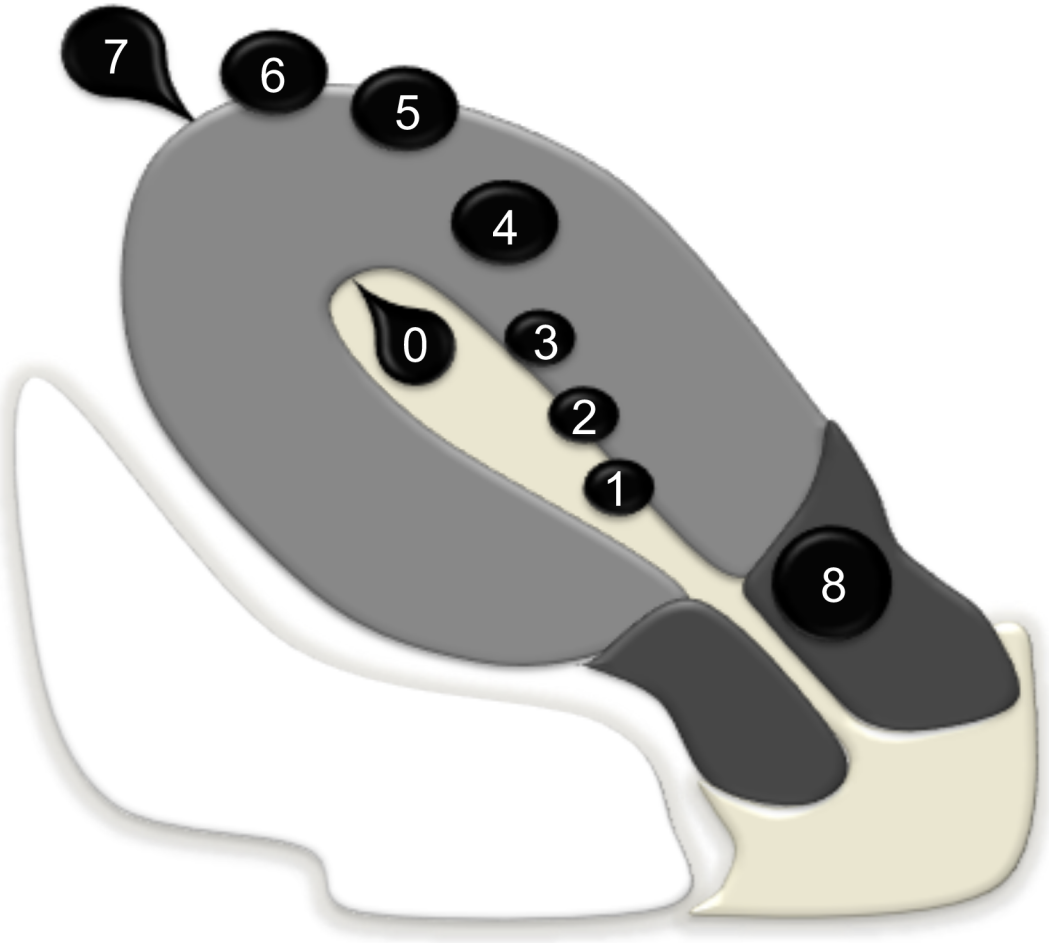
7
6
5
4
0
3
2
1
8

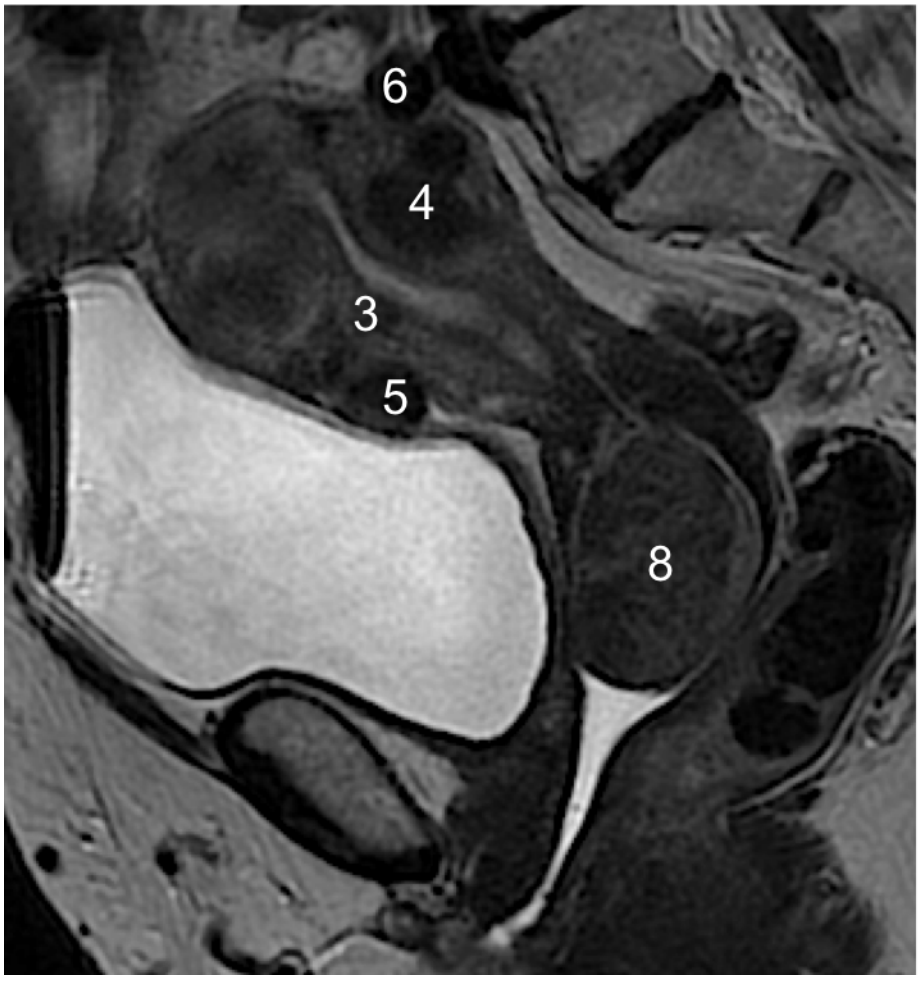
6
4
3
5
8

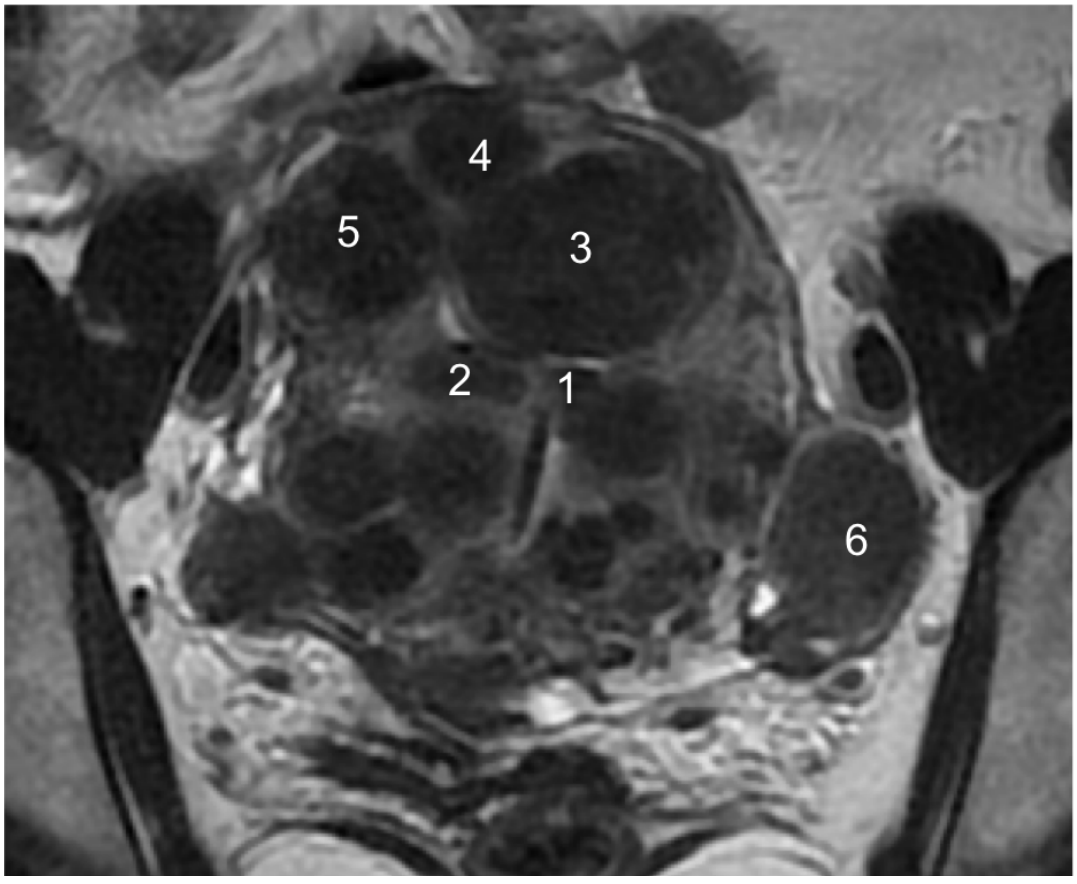
4
5
3
2
1
6

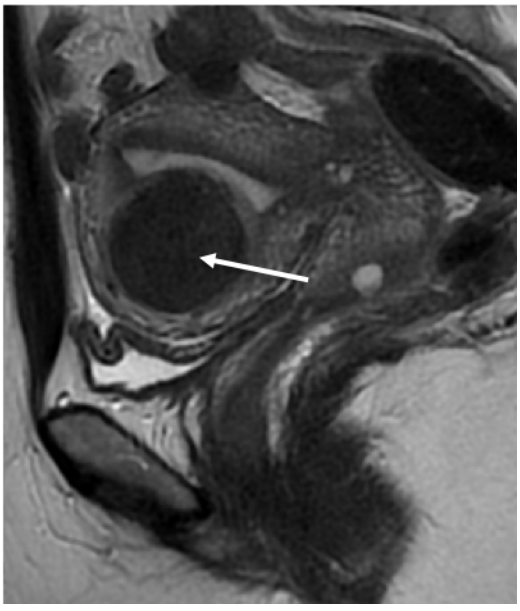

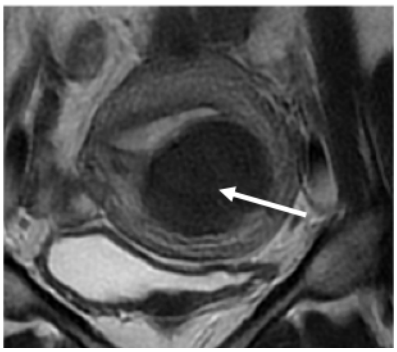

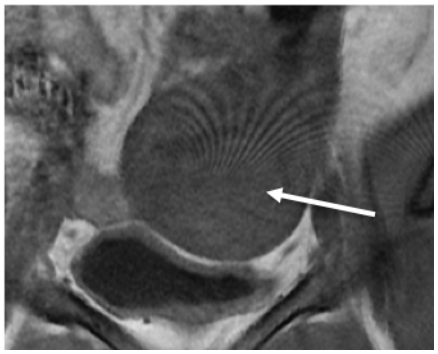

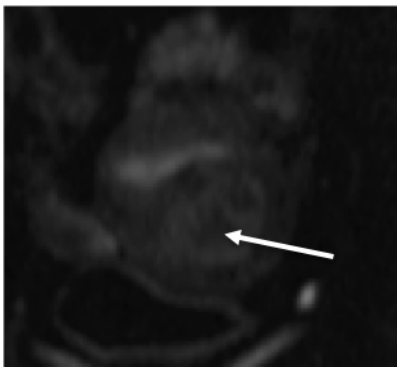

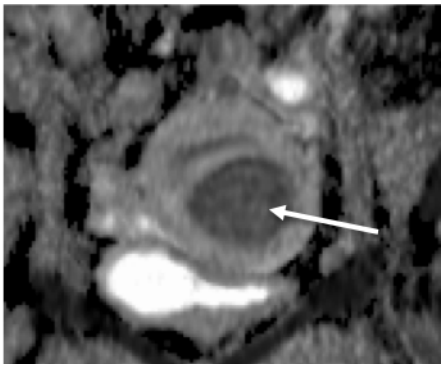

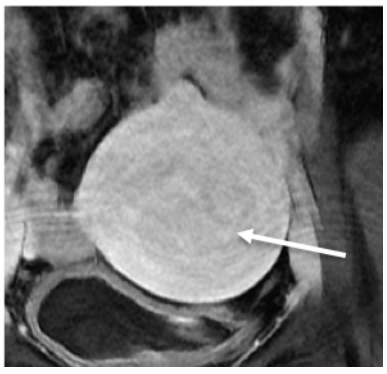

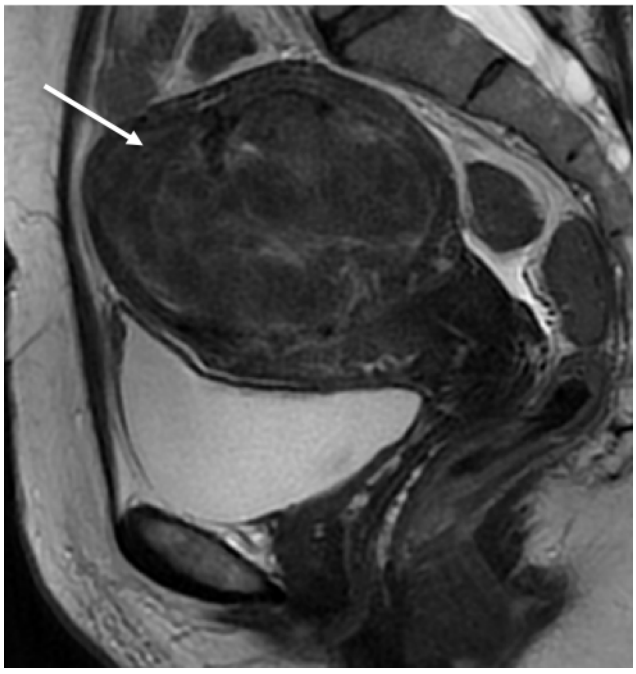

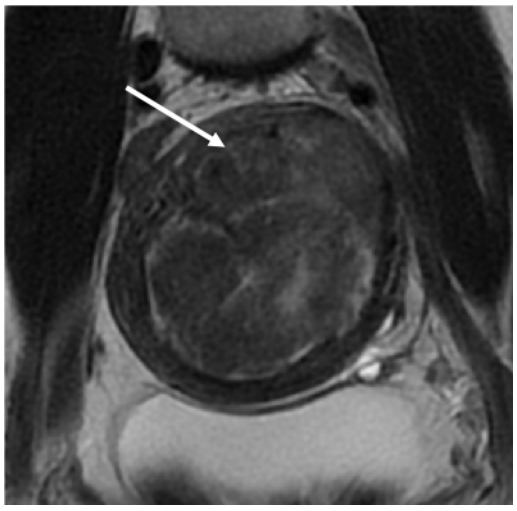

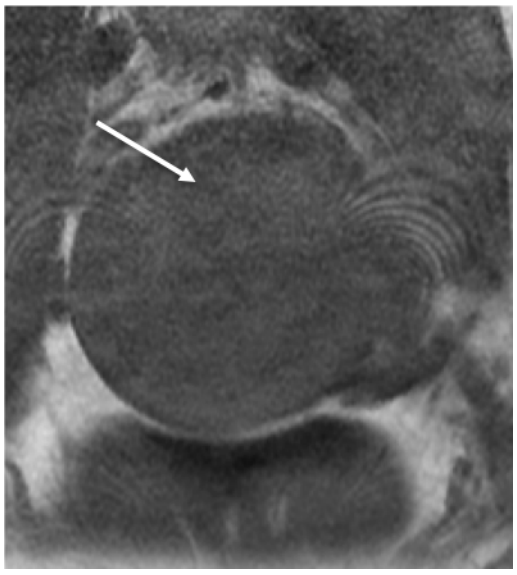

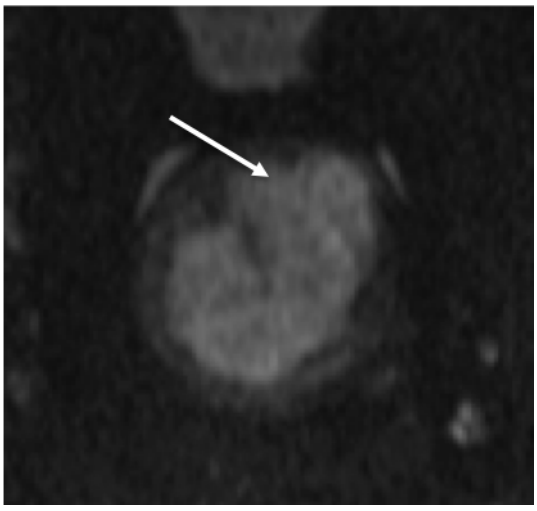

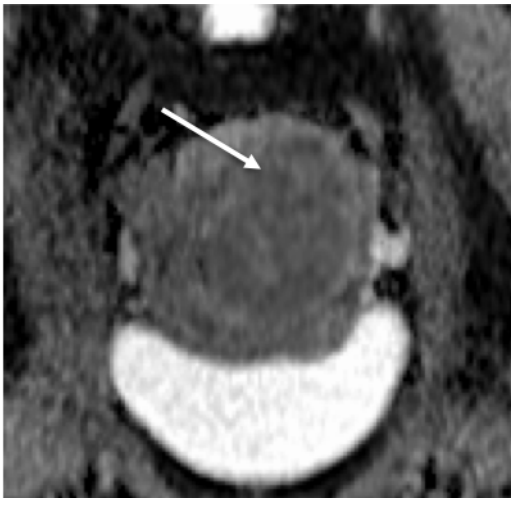

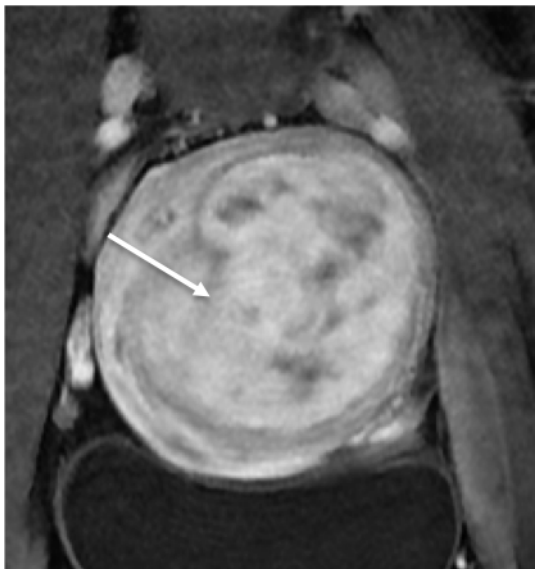

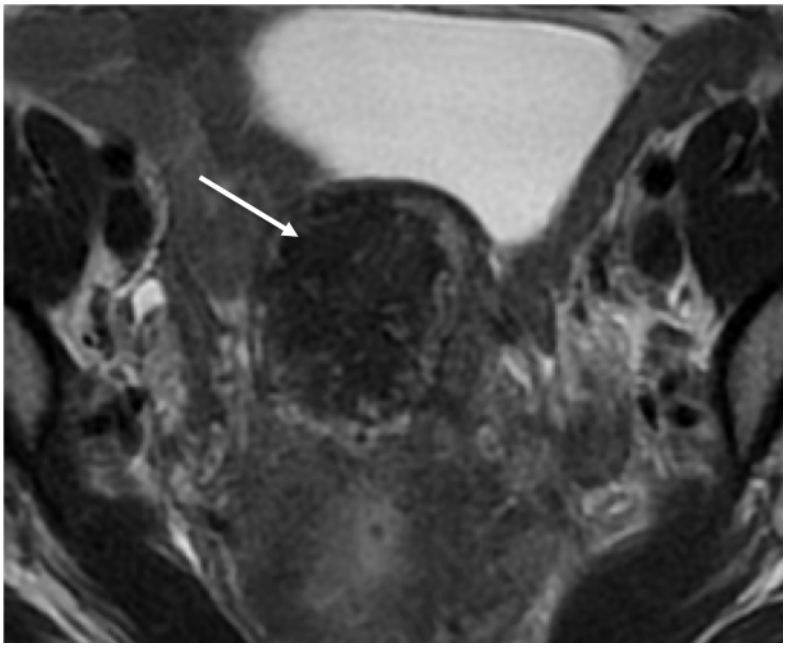

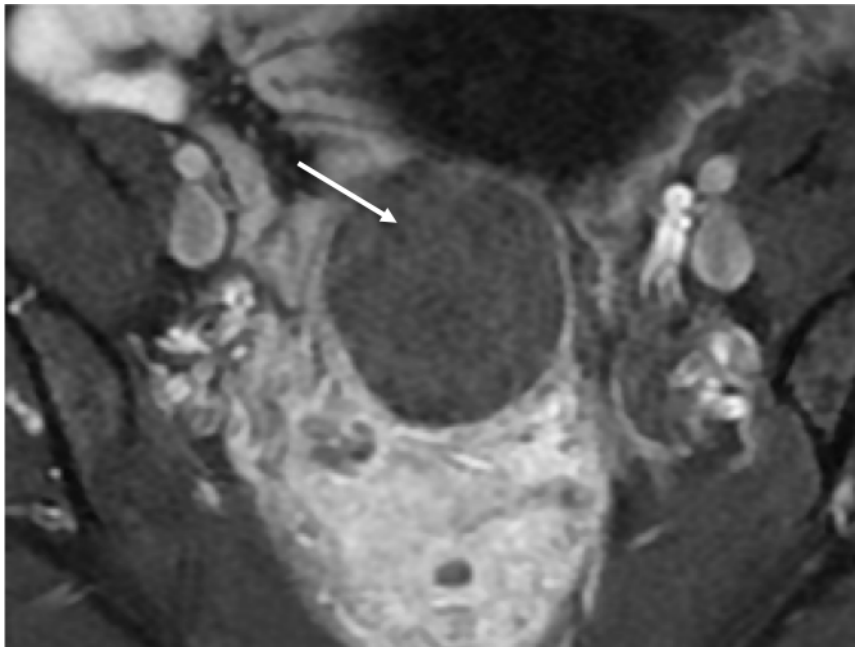

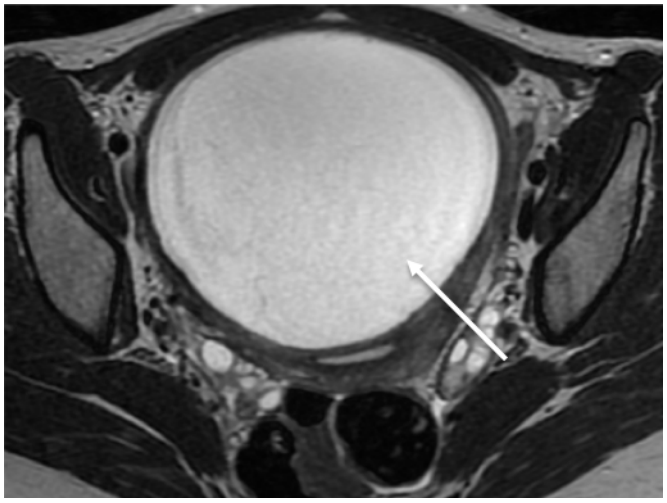

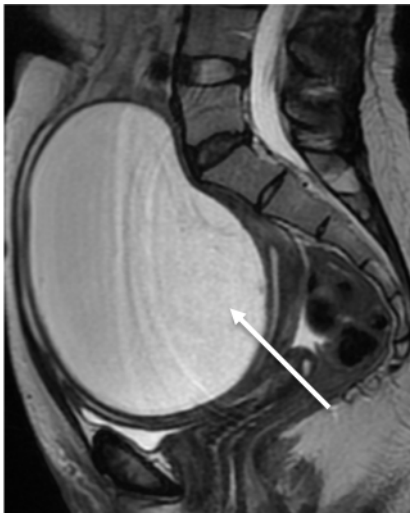

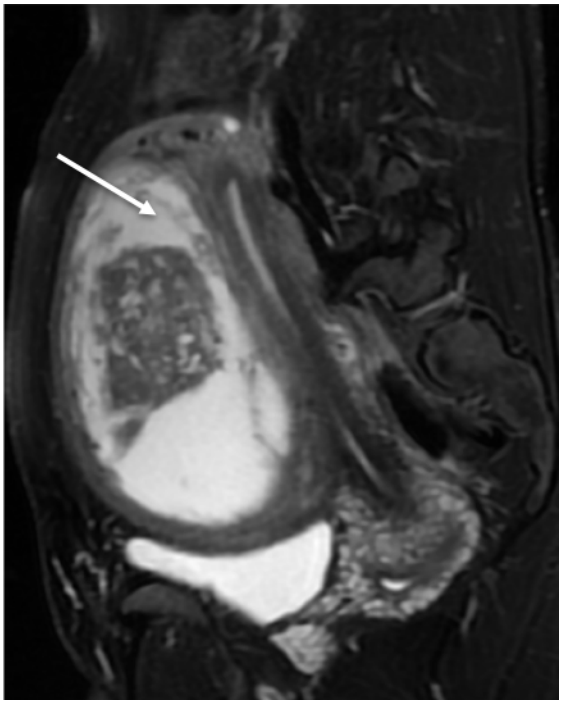

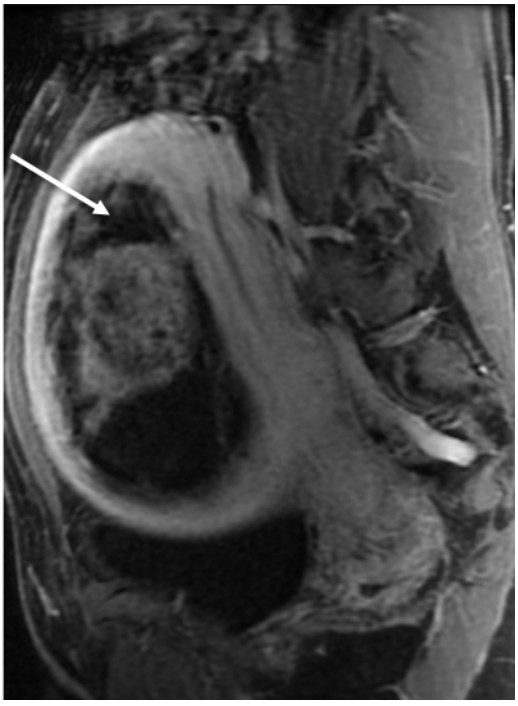

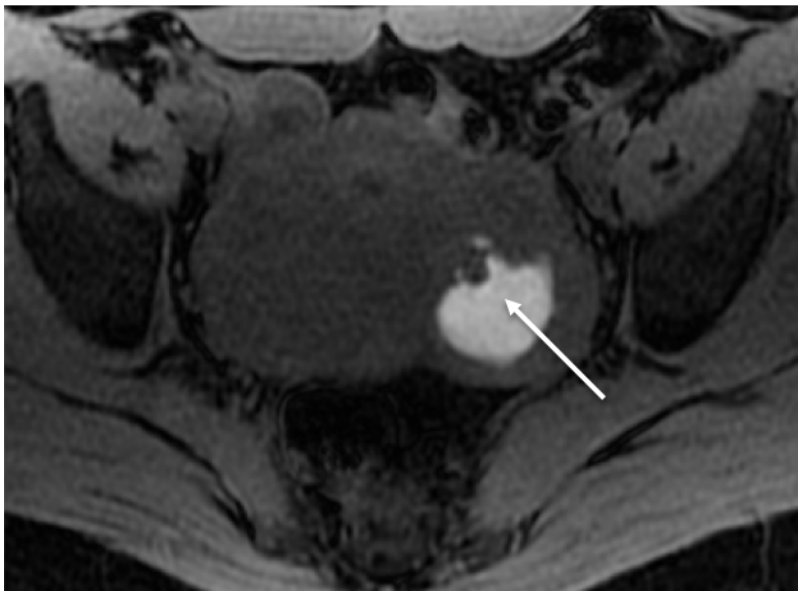

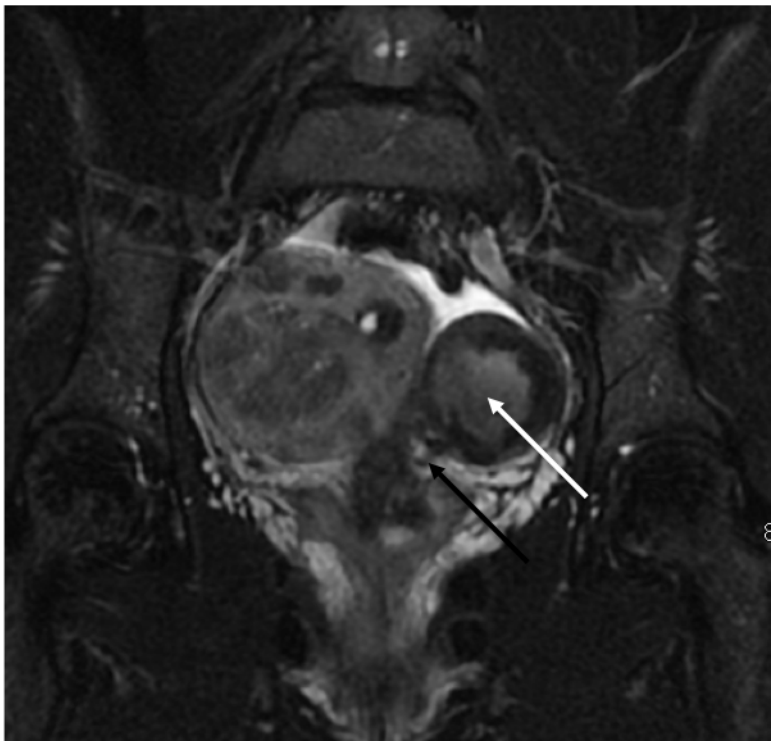

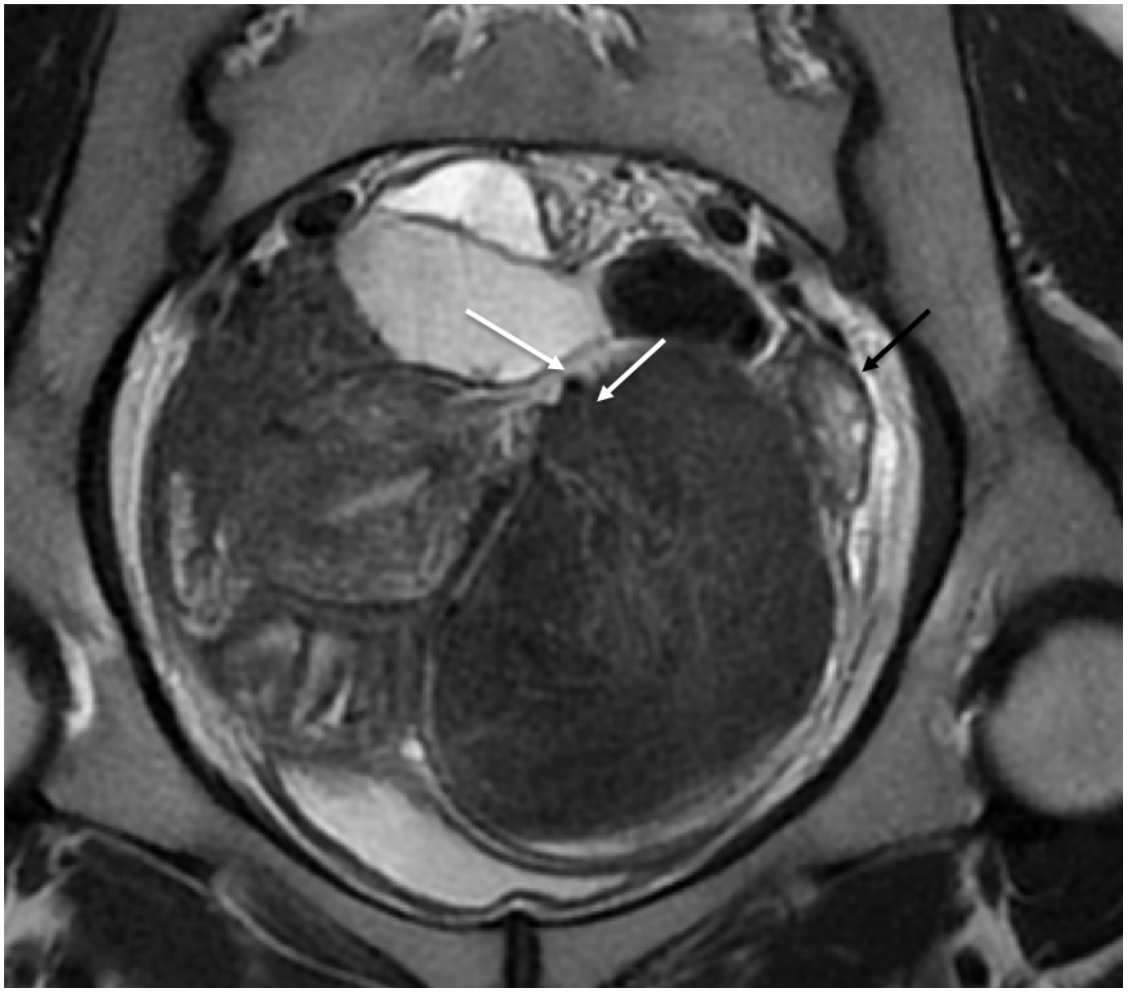

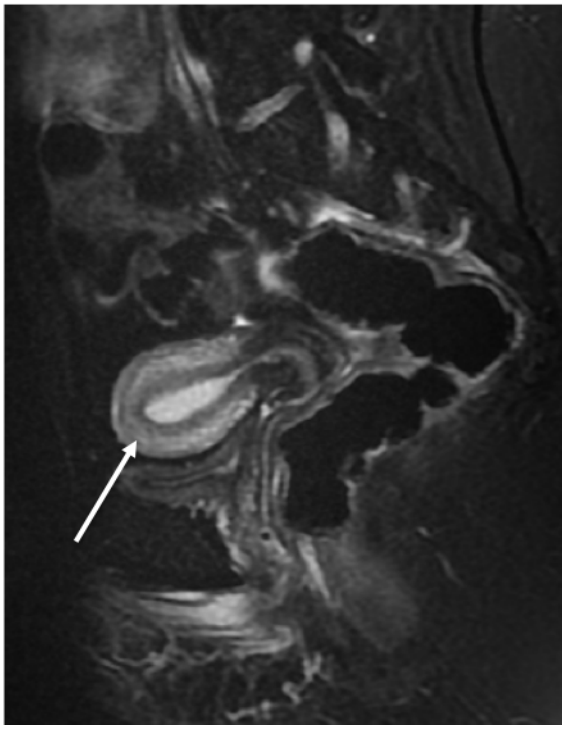

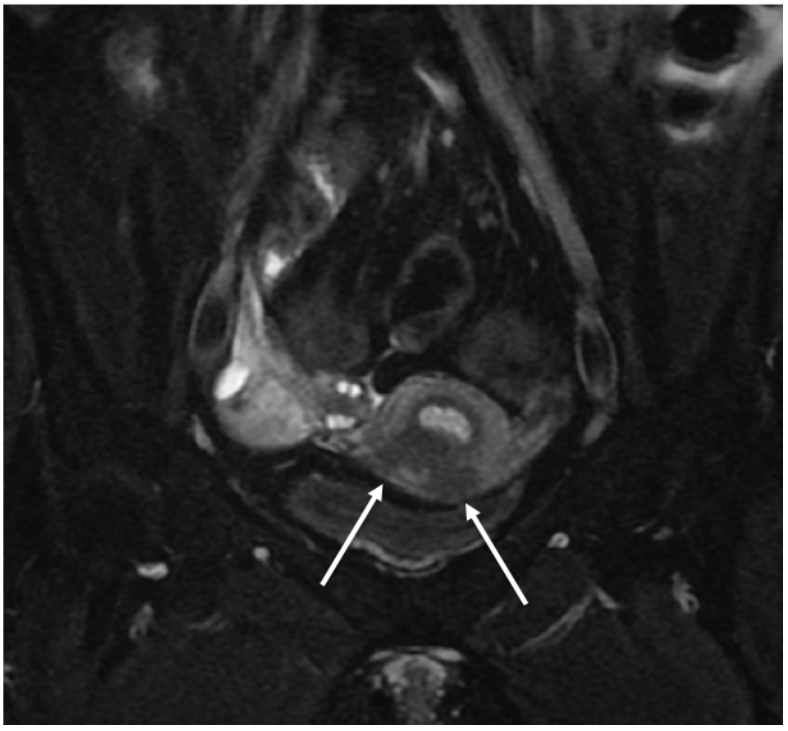

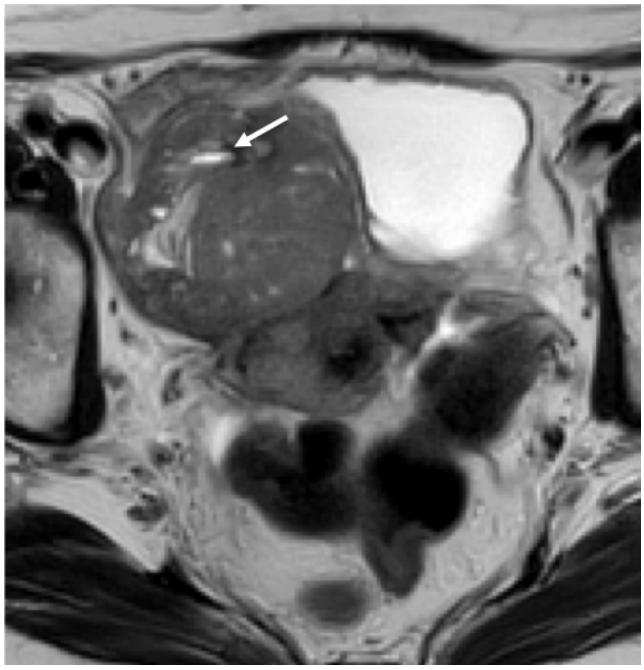

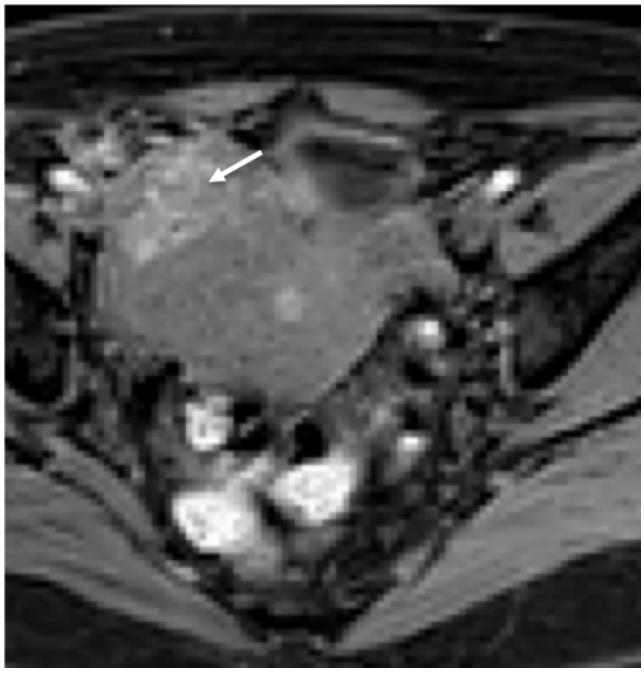

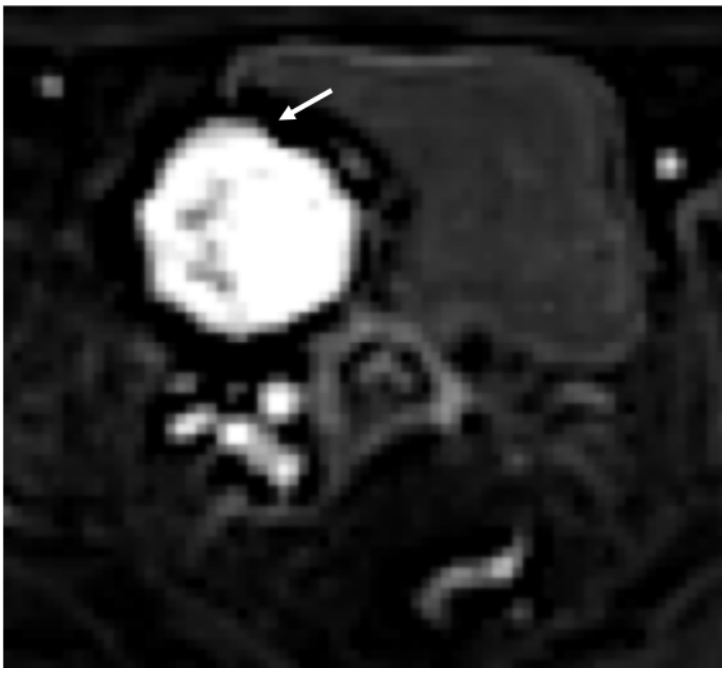

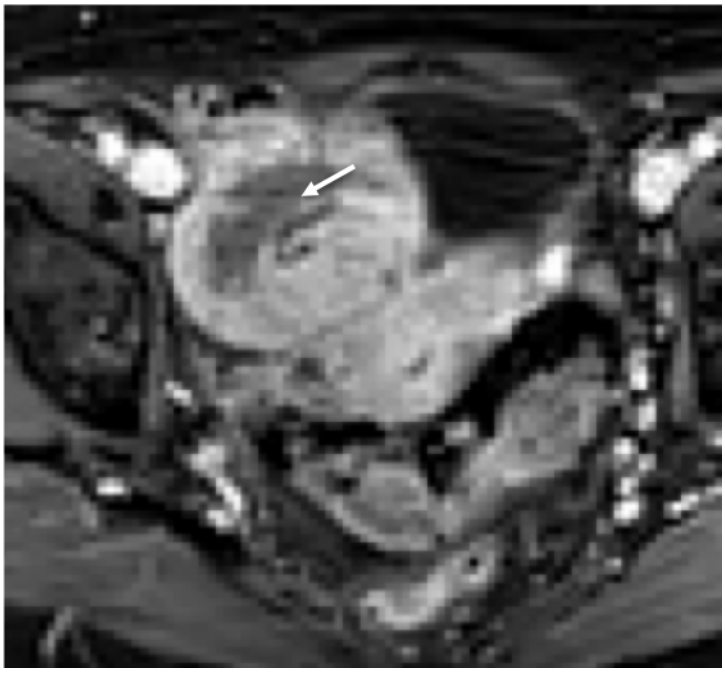

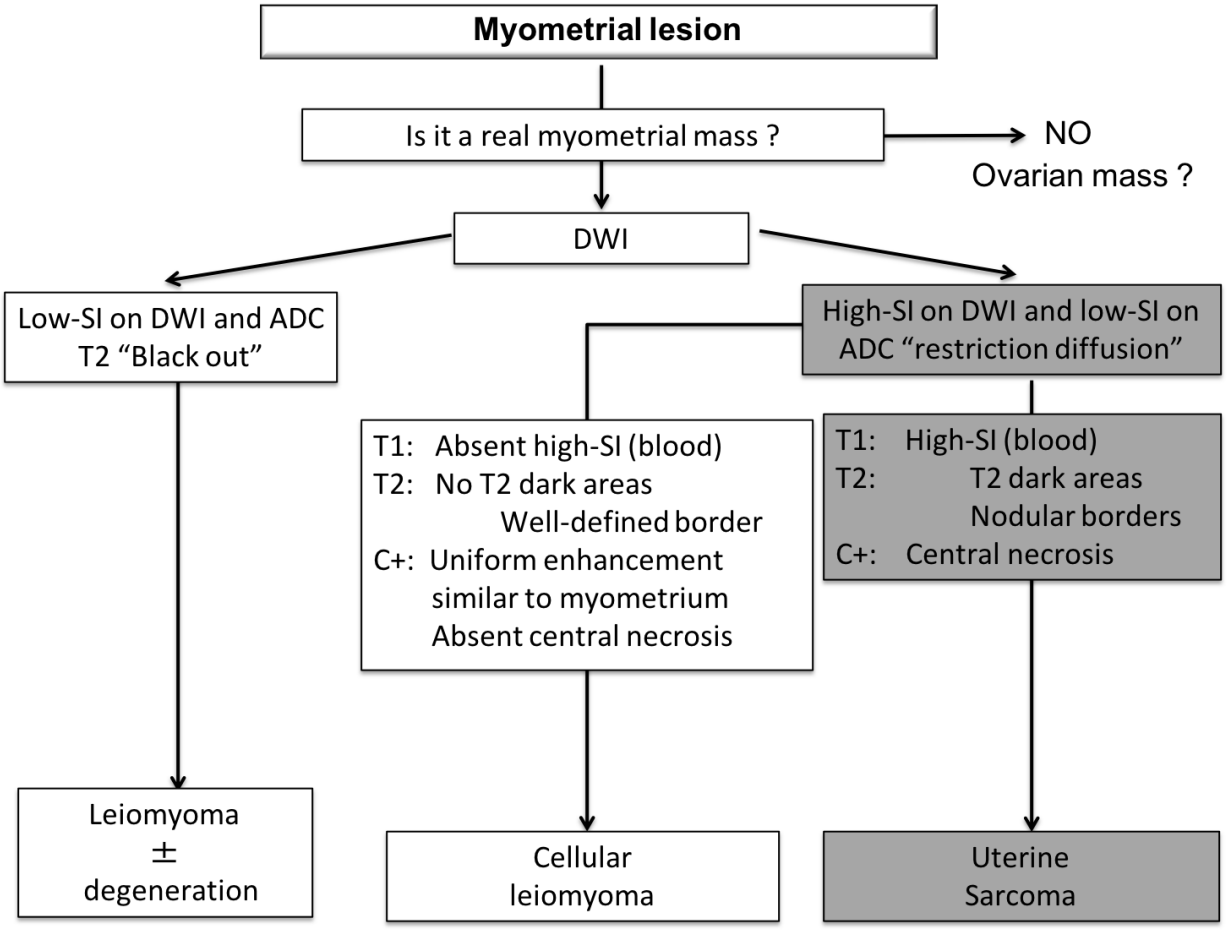
Myometrial lesion
Is it a real myometrial mass ?
NO
Ovarian mass ?
DWI
Low-SI on DWI and ADC
T2 "Black out"
High-SI on DWI and low-SI on
ADC "restriction diffusion"
T1: Absent high-SI (blood)
T2: No T2 dark areas
Well-defined border
C+: Uniform enhancement
similar to myometrium
Absent central necrosis
T1: High-SI (blood)
T2: T2 dark areas
Nodular borders
C+: Central necrosis
Leiomyoma
±
degeneration
Cellular
leiomyoma
Uterine
Sarcoma

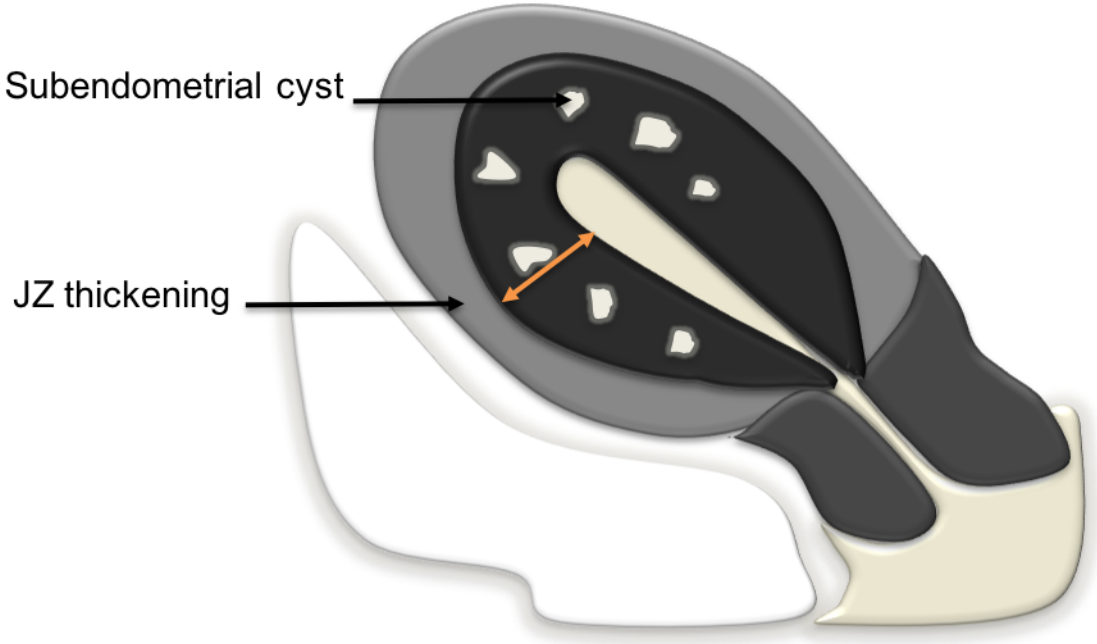
Subendometrial cyst
JZ thickening

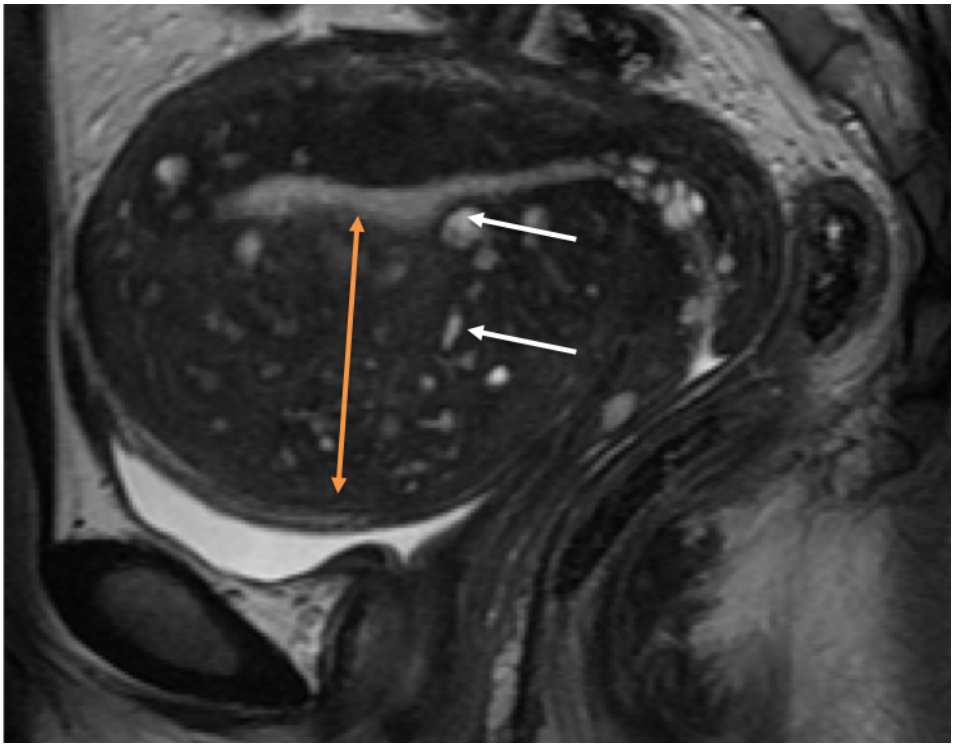

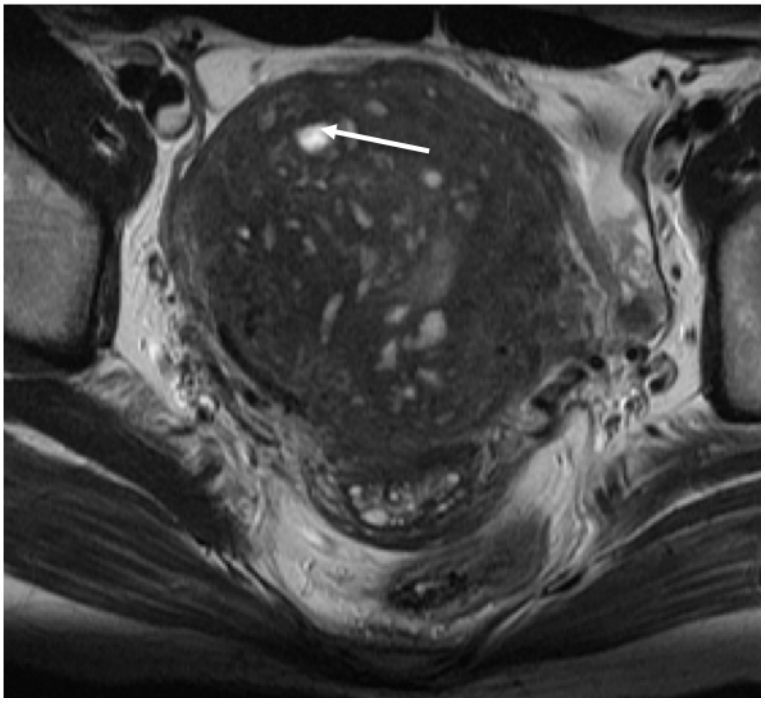

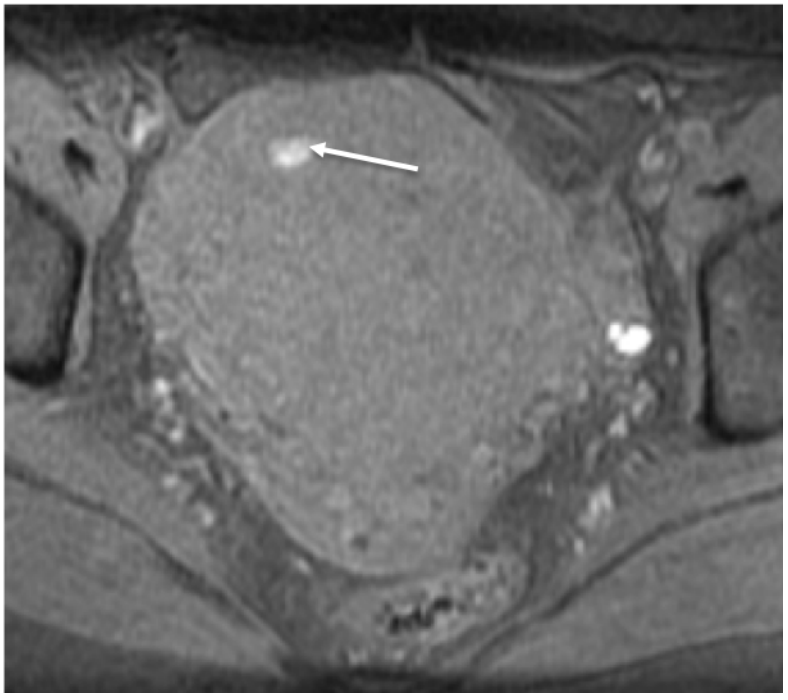

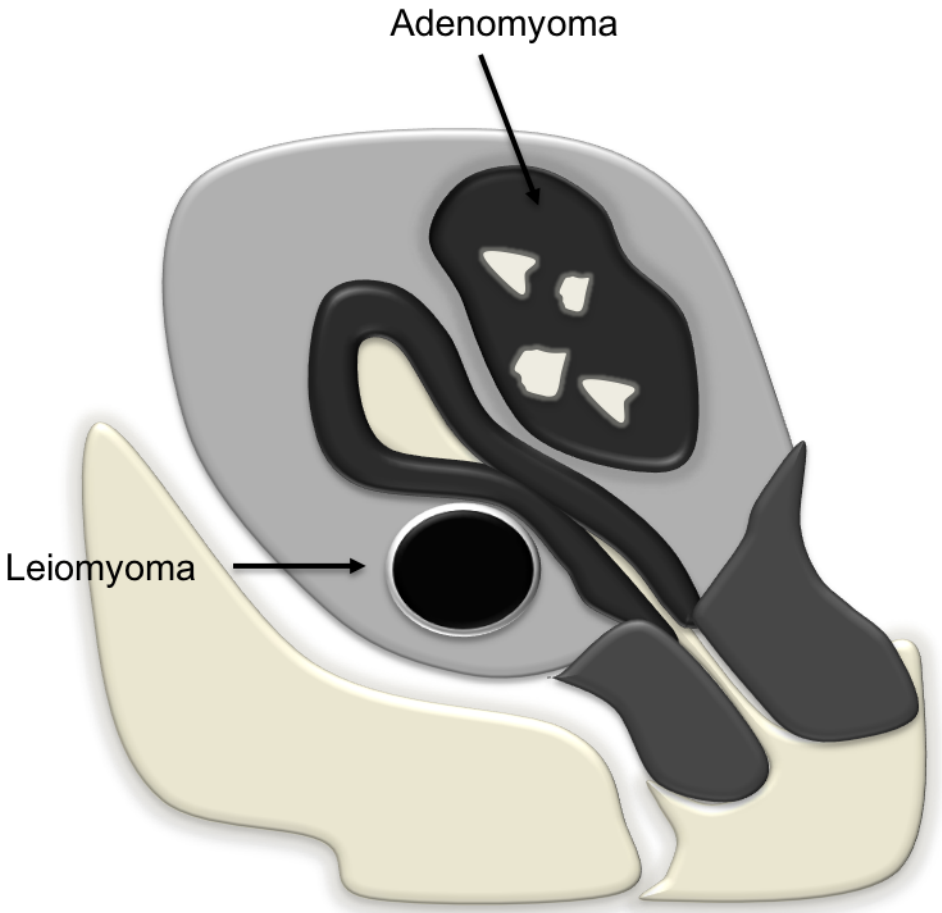
Adenomyoma
Leiomyoma

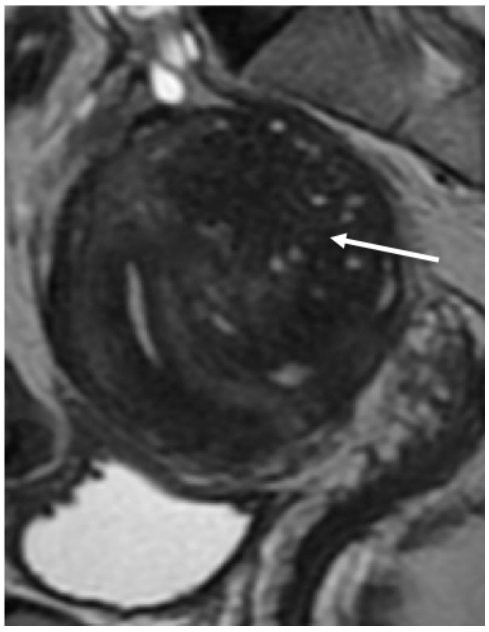

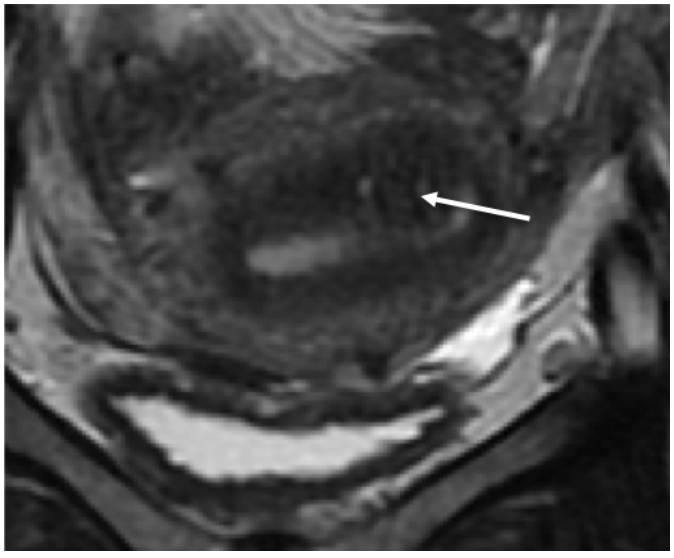

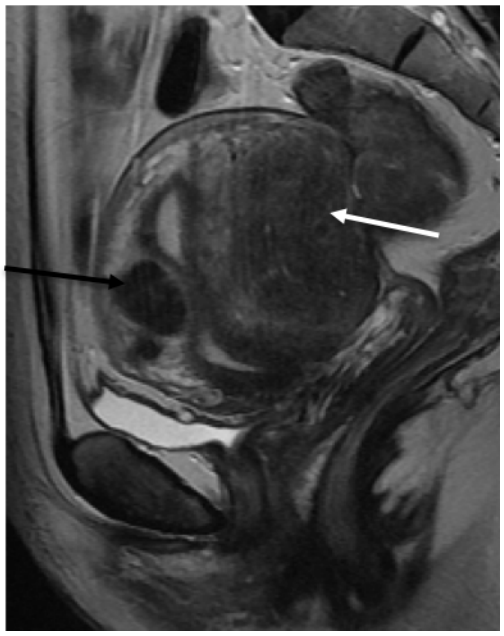

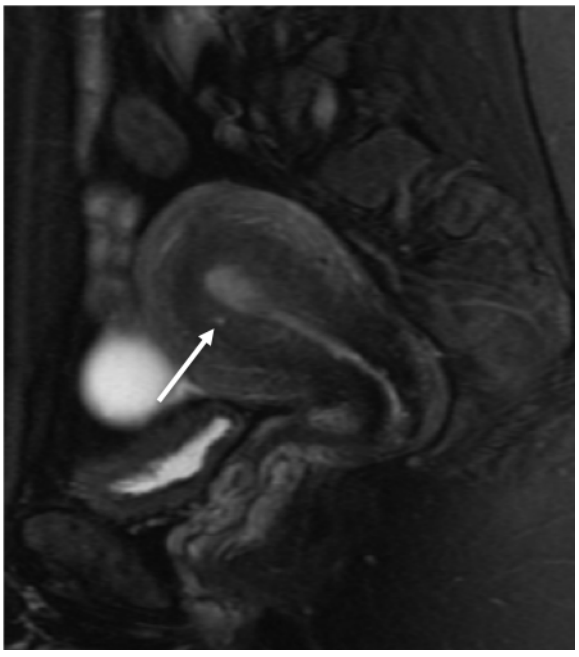

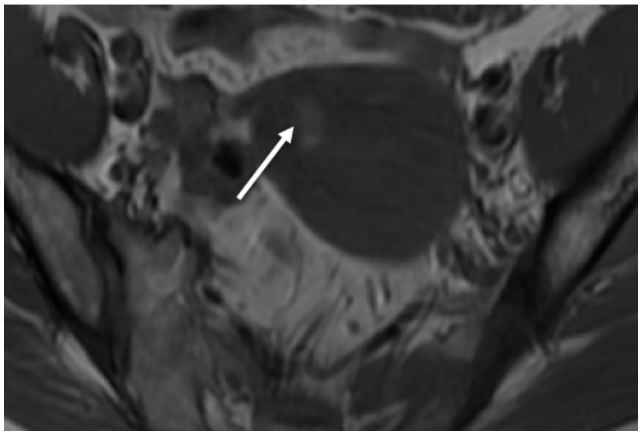

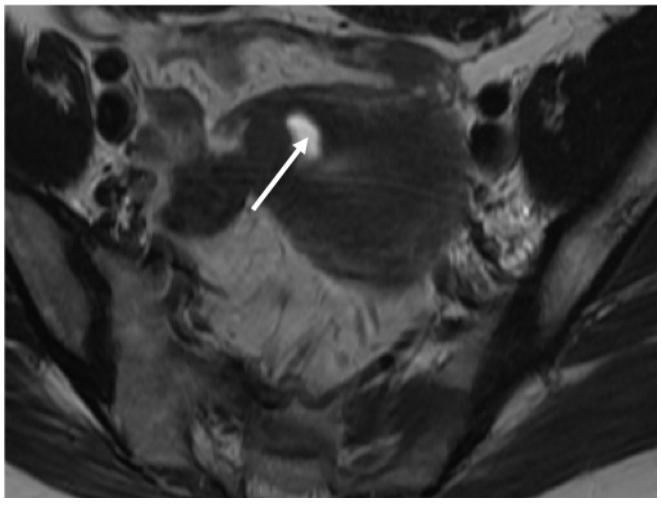

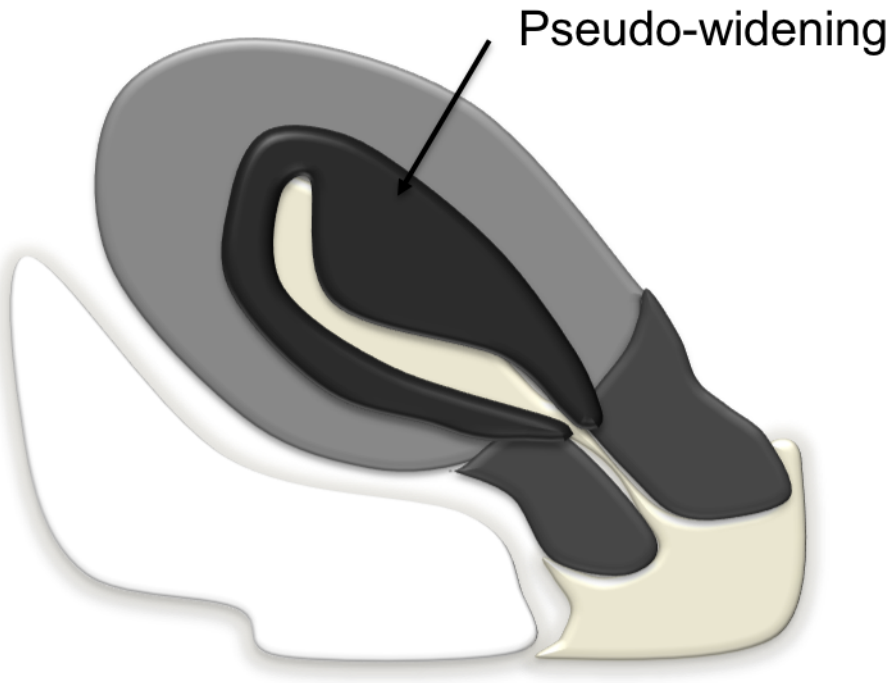
Pseudo-widening